Supplementary Figures

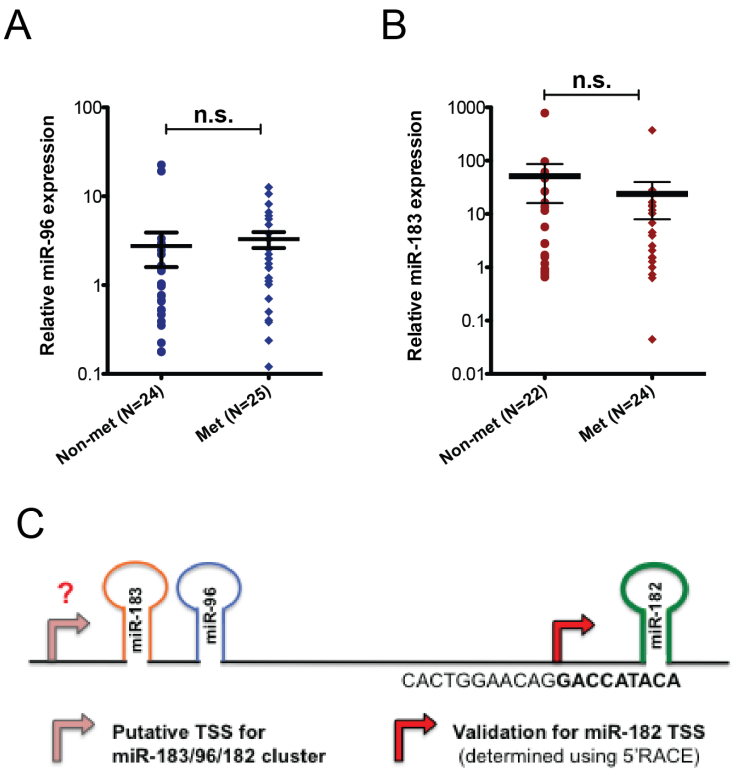

Supplementary Figure 1. miR-96 and miR-183 are not elevated in metastatic sarcomas. (**A&B**) No change in miR-96 and miR-183 expression in primary mouse STS was observed, measured by real time RT-PCR. (**C**) 5' RACE identified an independent promoter that drives miR-182 expression. All data are mean ± SEM.

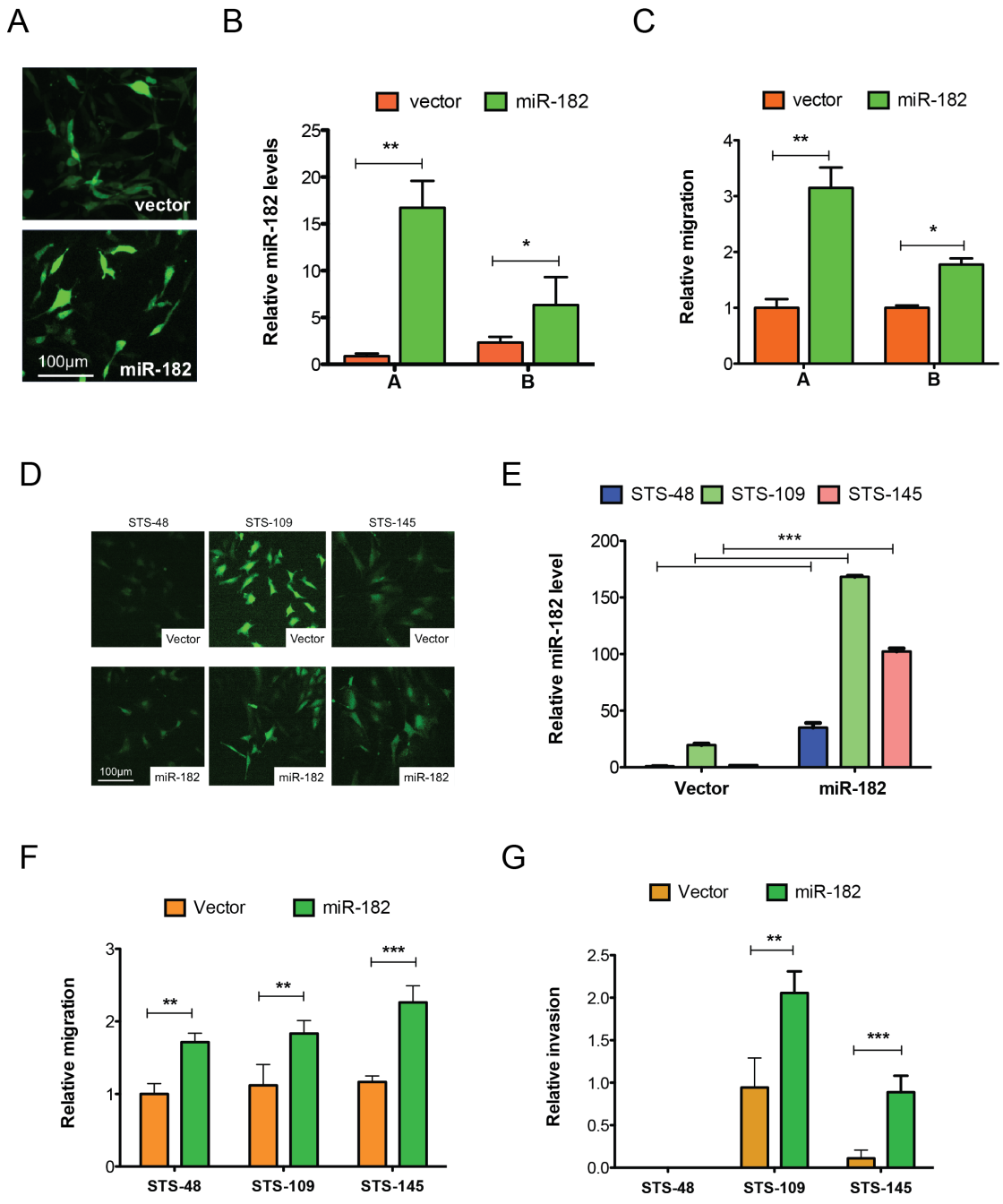

Supplementary Figure 2. miR-182 promotes cell migration and invasion of human sarcoma cells. (**A**) Image showing stably transduced sarcoma cell line expressing copGFP ± miR-182. (**B**) Real-time PCR confirming ectopic expression of stably transduced miR-182. (**C**) Overexpression of miR-182 increases migration in Transwell migration assay (n=3 independent experiments). (**D**) Images showing stably transduced human sarcoma cell lines expressing copGFP ± miR-182. (**E**) Real time RT-PCR validates overexpression of miR-182 in all human sarcoma cell lines compared to vector controls. (**F**) Overexpression of miR-182 increases migration and (**G**) invasion (n=6).

Two-way ANOVA is used for statistical analysis followed by Bonferroni post-hoc tests. All data are mean ± SEM. Scale bars: 100 μm (A and D). *P<0.05, **P<0.01, ***P<0.005.

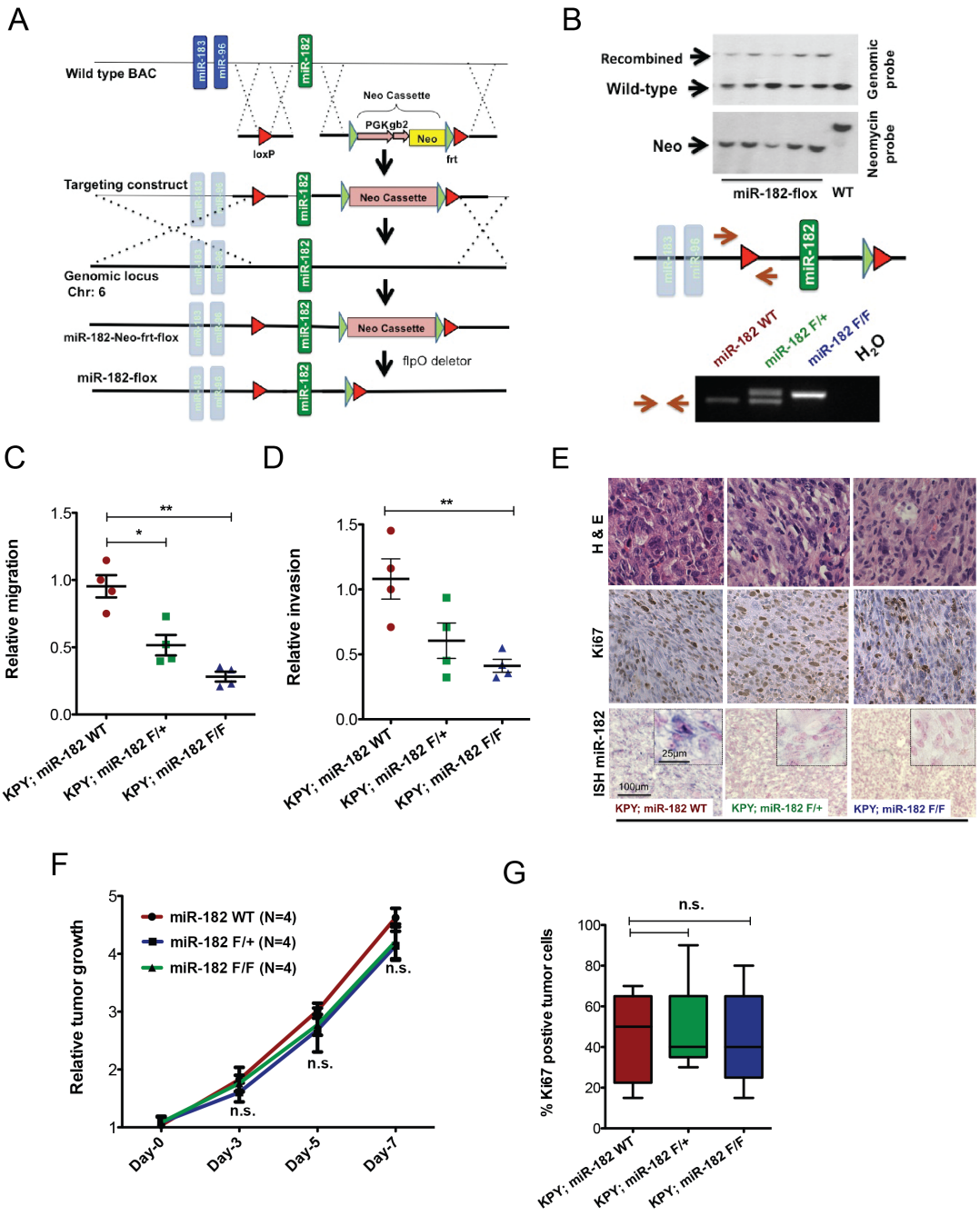

Supplementary Figure 3. Generation and validation of miR-182 conditional knockout mice. (**A**) Schematic of targeting constructs to generate genetically engineered mice with conditional knockout miR-182 (miR-182-flox). (**B**) Southern blot shows recombination of knock-in allele in ES cells (Top panel) and genotyping of mice demonstrates germline transmission of one or two copies of miR-182-flox allele (Bottom panel). (**C** & **D**) Quantification of Transwell migration assay and Matrigel invasion assay reveals that deletion of either one or two copies of miR-182 is sufficient to suppress migration and invasion of the cells (Four independent cell lines from each genotype were included for **C** & **D**. All of the experiments were performed in triplicate) . (**E**) *Top*

panel: Hematoxylin & Eosin (H & E) staining demonstrates that the deletion of miR-182 does not affect sarcoma histology. *Middle panel*: Ki67 staining suggests no significant change in proliferation of cells among different genotypes. *Bottom panel*: *ISH* detects lower miR-182 expression in primary sarcomas from KPY; miR-182-flox mice. (**F**) No change in tumor growth kinetics is observed with miR-182 deletion. (**G**) Quantification of Ki67 staining. Two-tailed student's t-test and One-way ANOVA, followed by Bonferroni post-hoc tests, is used for statistical analysis. All data are mean ± SEM.*P<0.05, **P<0.01. Scale bars: 100 μm in E; 25 μm (E, insets).

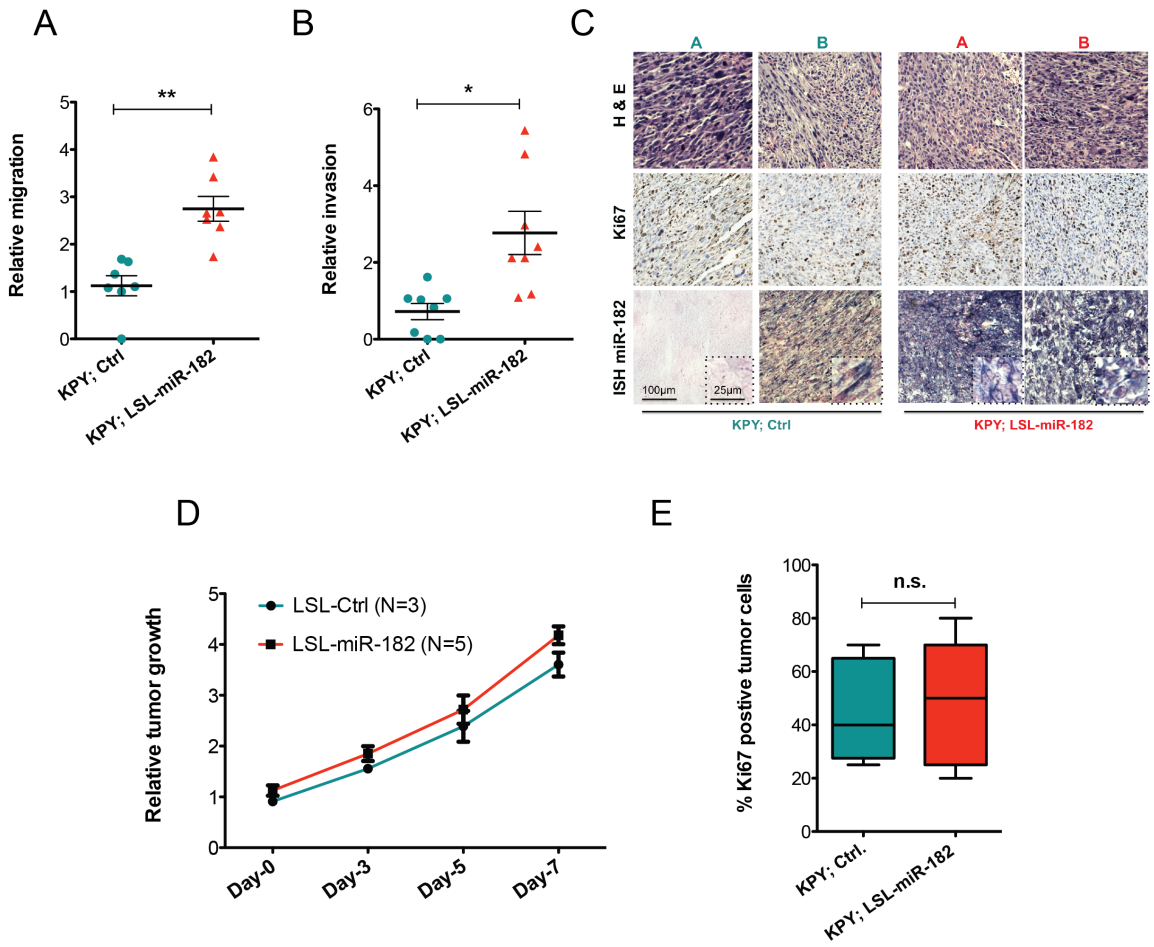

Supplementary Figure 4. miR-182 overexpression enhances cell migration and invasion of primary mouse sarcoma cells. (**A**) Quantification of Transwell migration assay and (**B**) Matrigel invasion assay shows that overexpression of miR-182 is sufficient to increase both migration and invasion of the primary sarcoma cells, respectively (n=8). (**C**) *Top panel*: Hematoxylin & Eosin (H & E) staining demonstrates that the overexpression of miR-182 does not affect sarcoma histology. *Middle panel*: Ki67 staining suggests no significant change in proliferation of cells among different genotypes. *Bottom panel*: *ISH* detects higher miR-182 expression in primary sarcomas from KPY; LSL-miR-182 mice. (**D**) No difference in tumor growth kinetics is observed with miR-182 overexpression. (**E**) Quantification of Ki67 staining. Student's t-test and One-way ANOVA is used for statistical analysis. All data are mean ± SEM. *P<0.05, **P<0.01. Scale bars: 100 μm in C; 25 μm (C, insets).

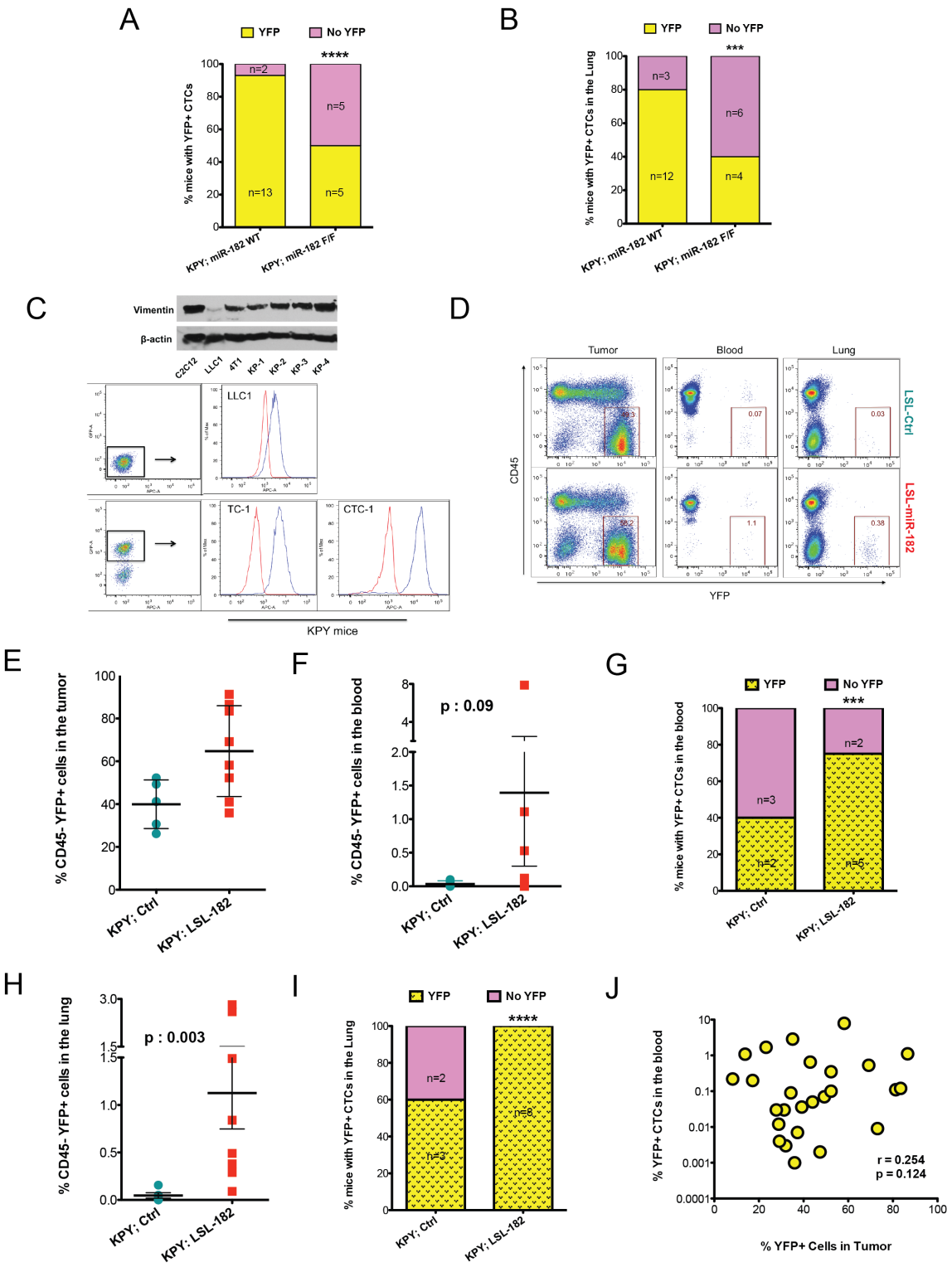

Supplementary Figure 5. miR-182 controls both intravasation and extravasation of sarcoma cells. (**A** & **B**) Quantification of CD45- YFP+ cells within the blood and lung between the two genotypes. (**C**) *Upper panel*: Western blot detects vimentin expression in primary mouse KP sarcoma cells lines (Numbered KP-1 through 4). C2C12: mouse

myoblast, LLC1: Lewis lung carcinoma and 4T1: mouse breast carcinoma cell line. *Lower panel:* Flow cytometry showing YFP+ primary KP cells (TC-1) and CTCs (CTC-1) are positive for vimentin (APC-labelled). *Red histogram*: IgG isotype and *Blue histogram*: vimentin staining. (**D**) Flow cytometry showing number of YFP+ cells in the tumor, blood and lung after miR-182 overexpression. (**E**) Quantification of CD45- YFP+ cells in primary tumors between the two genotypes. (**F**,**G,H & I**) Quantification of CD45- YFP+ cells within the blood and the lungs between the two genotypes (N=8). (**J**) No correlation is observed between the percentage of CD45- YFP+ cells in the tumor and CTCs. Two-tailed student's t-test and Fisher's exact test were used for statistical analysis. All data are mean ± SEM *P<0.05, ***P<0.005

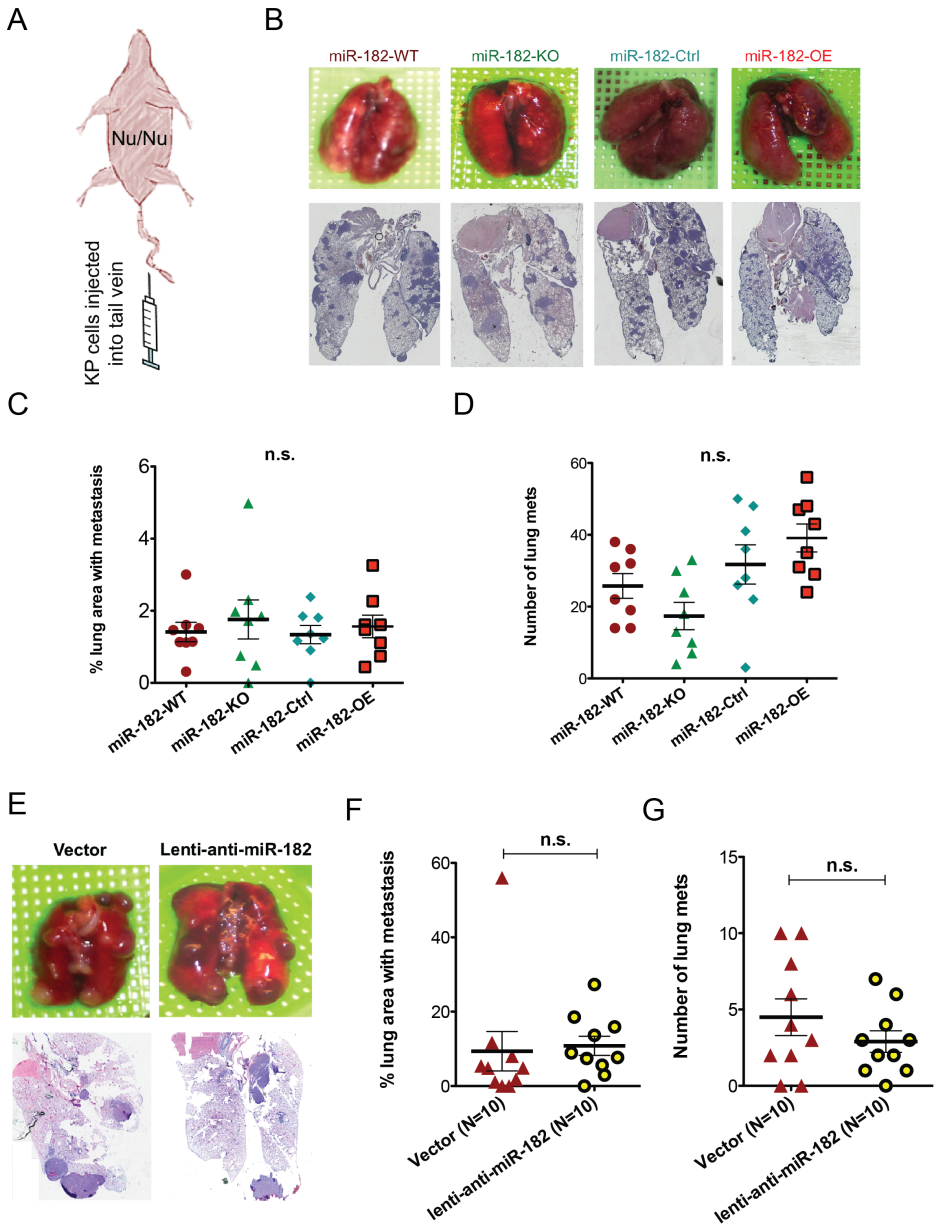

Supplementary Figure 6. miR-182 does not affect lung colonization following tail vein injections. (**A**) Schematic showing experimental metastasis assay. (**B**) Gross lung images (Top) and lung histology (Bottom) showing metastatic nodules among different genotypes. (**C**) Quantification of the number of lung metastases and (**D**) percentage of lung area with metastasis revealed no significant difference among different genotypes in an experimental metastasis assay. (**E**) Gross lung images (Top) and lung histology (Bottom) showing metastatic nodules between vector and lenti-anti-miR-182. (**F**) Quantification of the number of lung metastases and (**G**) percentage of lung area with metastasis revealed no significant difference between the two genotypes. Notably, the same sarcoma cell line with stable miR-182 knockdown showed a significant difference

in both the number of lung metastases and percentage of lung area with metastasis when injected orthotopically in mice (Refer to Fig 2). One-way ANOVA and two-tailed student's t-test is used for statistical analysis. All data are mean ± SEM. Magnification: All lungs were scanned with a 2.5X objective using Leica DM5500B microscope.

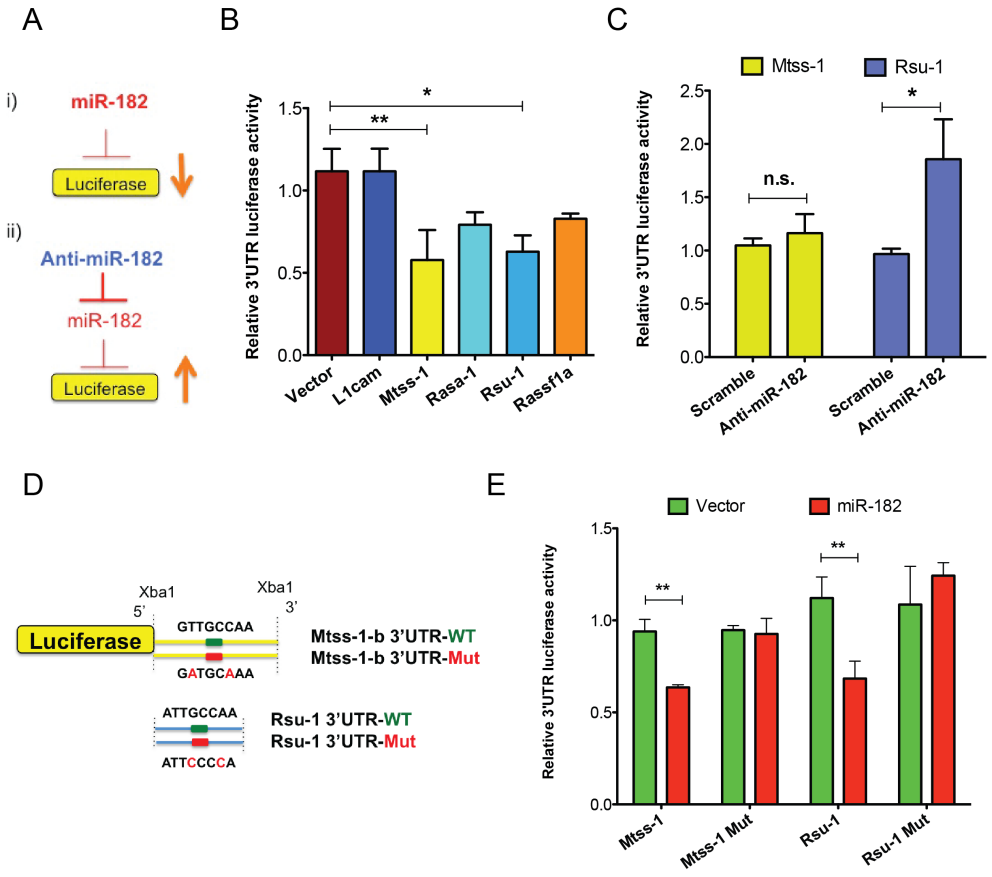

Supplementary Figure 7. *In silico* / 3'UTR luciferase screens predict Rsu-1 and Mtss-1 as miR-182 targets. (**A**) Schematic shows the principle of the luciferase reporter assay. (**B**) Luciferase assay shows decreased luciferase reporter activity of Rsu-1 and Mtss1 with miR-182 overexpression and (**C**) increased expression with miR-182 knockdown in HEK-293T cells (n=3). (**D**) Schematic showing alignment of Mtss-1 and Rsu-1 3'UTR binding motif with miR-182. Wild-type binding motifs (Green) are mutated to red sequences. (**E**) Luciferase assay shows no suppressive effect for mutant UTR clones with miR-182 overexpression. One-way ANOVA (B) and two-way ANOVA (C&E) were used for statistical analysis. All data are mean ± SEM. *P<0.05, **P<0.01.

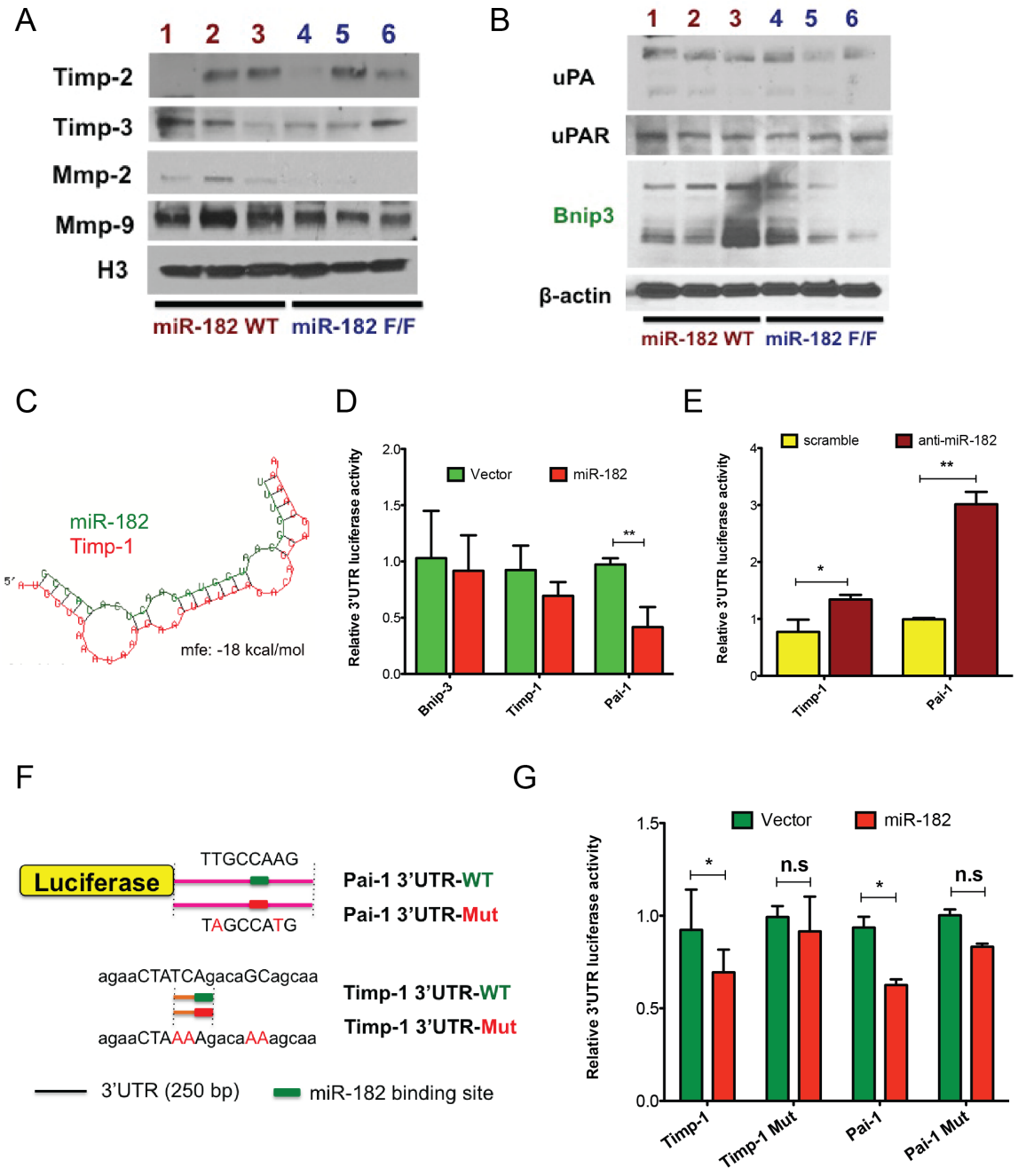

Supplementary Figure 8. Luciferase reporter assay confirms Pai-1 and Timp-1 as direct targets of miR-182. (**A**) No change in Timp-2, Timp-3 and MMP-9 proteins was observed, yet activated MMP-2 was decreased in miR-182 deleted cells. Timp-2 and Timp-3 are of interest because they have a miR-182 binding site in their 3'UTRs. (**B**) No change in endogenous uPA and uPAR proteins were seen in miR-182 deleted cells. uPAR was assessed because it interacts with both uPA and Pai-1. Despite being upregulated 3.5 fold in the proteomic screen, Bnip-3 is not validated as a miR-182 target by western blotting. (**C**) A weak miR-182 binding site on Timp-1 3'UTR is predicted by

RNA-Hybrid database. Interestingly, *RNA-Hybrid* predicted couple of miR-182 binding sites in 5'UTR and exon of Timp-1 (data not shown). (**D**) Luciferase assay shows decreased luciferase reporter activitiy of both Pai-1 and Timp-1 with miR-182 overexpression while (**E**) increased luciferase reporter activitiy with miR-182 knockdown. *Targetscan* predicts one miR-182 binding site each in Bnip-3 and Pai-1 3'UTRs, however does not predict any canonical binding site for miR-182 in the Timp-1 3'UTR. (**F**) Schematic showing alignment of Pai-1 and Timp-1 3'UTR binding motif with miR-182. Wild-type motifs (Green) are mutated to red sequences, respectively. (**G**) Luciferase assay shows no significant suppressive effect for mutant UTR clones with miR-182 overexpression. Two-way ANOVA was used for statistical analysis. All data are mean ± SEM *P<0.05, **P<0.01.

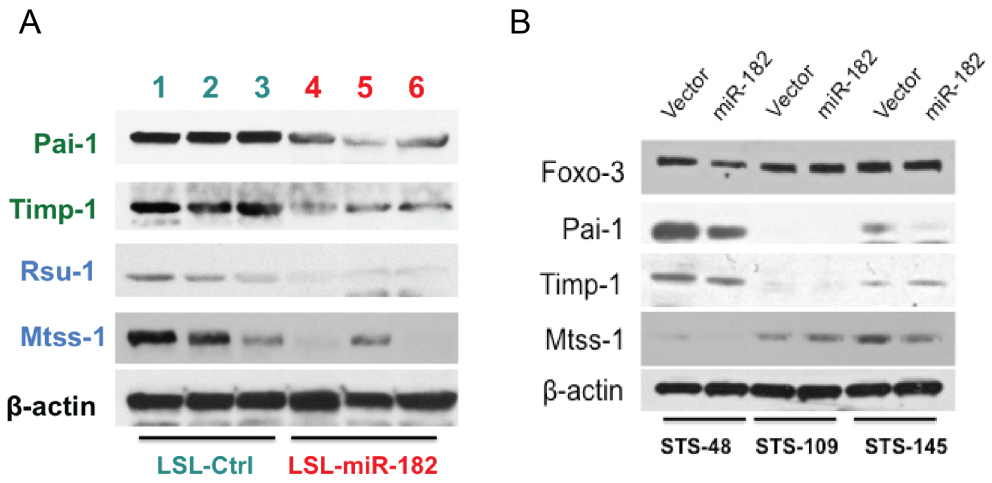

Supplementary Figure 9. miR-182 targets Pai-1, Timp-1, and Mtss-1 in human sarcoma cell lines. (**A**) Western blot validates downregulation of miR-182 targets Pai-1, Timp-1,Rsu-1 and Mtss-1 in primary cell lines derived from sarcomas miR-182 overexpressor mice and (**B**) in miR-182 overexpressing human sarcoma cell lines. Notably, Pai-1 and Timp-1 are undetectable in human cell line STS-109, which expresses 20-fold higher miR-182 than STS-48 and STS-145 (Supplementary Figure 2A). This further supports miR-182 regulation of Pai-1 and Timp-1. Rsu-1 was not detected in the human samples with the available antibody.

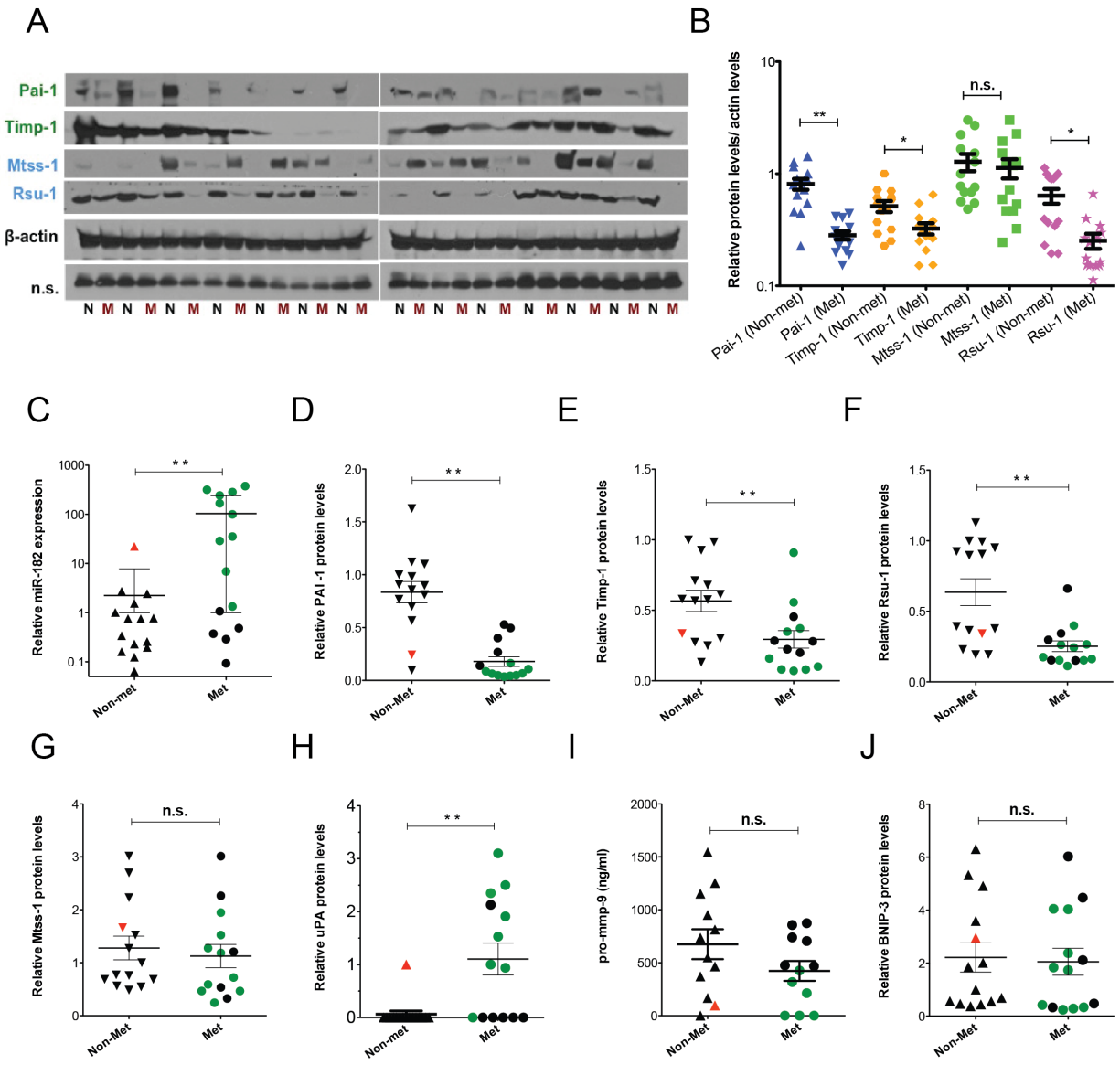

Supplementary Figure 10. Expression of proteases is elevated in primary mouse metastatic sarcomas. (**A**) Western blot performed on cell lysates from primary sarcomas with both metastatic (M) and non-metastatic (N) outcome having wild-type miR-182. (**B**) Quantification of western blot in **A**. (**C-I**) Graphs show differential mRNA expression of miR-182 and protein expression of Pai-1, Timp-1, Rsu-1 and Mtss-1 in metastatic and non-metastatic sarcomas. The metastatic sarcomas with high miR-182 expression are denoted in green circles and a single non-metastatic sarcoma with high miR-182 expression is denoted by a red triangle. These colored samples are followed through panels C-J to correlate miR-182 expression with the level of its targets. The Urokinase (uPA- **H**) and (**I**) pro-MMP-9 were detected using ELISA in primary metastaic KP sarcomas compared to non- metastatic sarcomas. (**J**) Quantification of western blot shows no difference in Bnip-3 protein, a miR-182 target predicted by *in silico* screen.

Two-tailed student’s t-test was used for statistical analysis. All data are mean ± SEM **P<0.01.

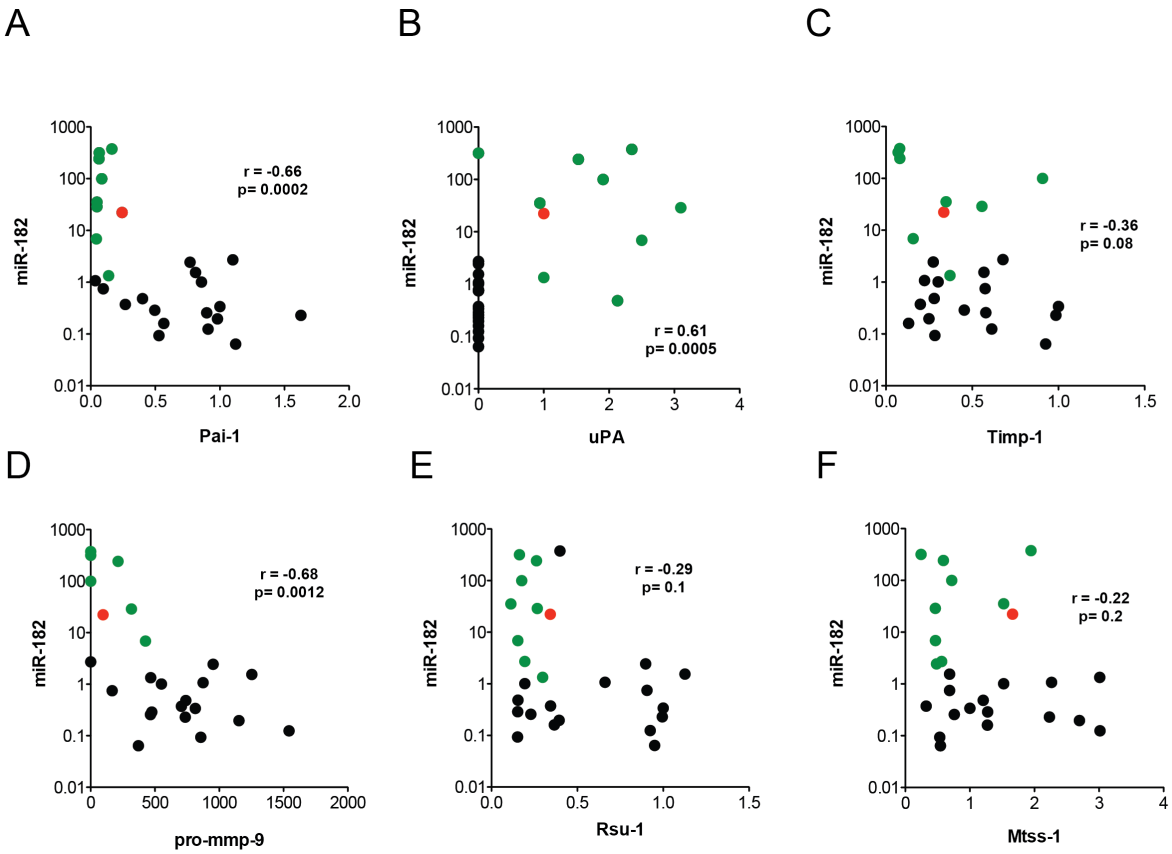

Supplementary Figure 11. miR-182 expression correlates with protein expression of Pai-1, uPA, Timp-1, pro-MMP-9, Rsu-1 and Mtss-1 in primary mouse sarcomas. (**A**, **D**, **E** & **F**) miR-182 levels negatively correlate with protein levels of its target genes such as Pai-1, Timp-1, Rsu-1 and Mtss-1 in primary sarcomas. (**B**) miR-182 levels positively correlates with the amount of urokinase (uPA) in primary sarcomas. (**C**) miR-182 levels also negatively correlate with protein levels of pro-MMP-9 within the primary sarcomas. Refer to figure 4 for designation of the color scheme. Spearman (r) correlation test was used for statistical analysis.

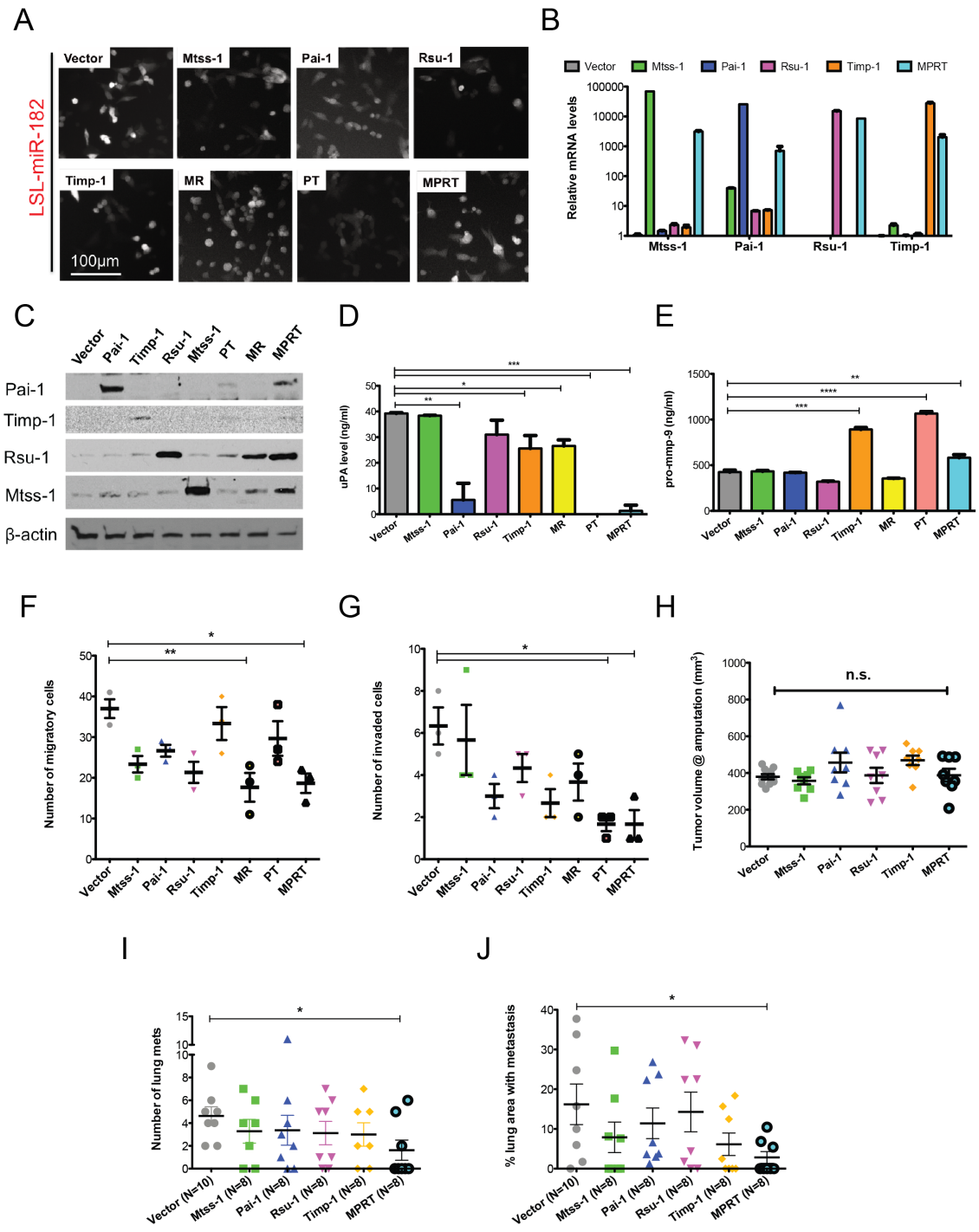

Supplementary Figure 12. Generation and characterization of primary KP; LSL-miR-182 cell line ectopically expressing miR-182 targets. (**A**) Images showing stably transduced KP; LSL-miR-182 cell line expressing copGFP ± either Mtss-1, Pai-1, Rsu-1, Timp-1, Mtss-1 and Rsu-1 (MR), Pai-1 and Timp-1 (PT) or in combination (MPRT). (**B & C**) Real-time PCR and western blot confirming ectopic expression of stably transduced

target genes either alone or in combination, respectively. (**D & E**) ELISA confirming significant modulation of uPA and pro-MMP-9 in the Pai-1 and Timp-1 transduced cells. (**F**) Effects of overexpression of Mtss-1, Pai-1, Rsu-1, Timp-1, MR, PT or MPRT on migration and (**G**) invasion of primary KP; LSL-miR-182 cells, as assessed by Transwell migration assay and Matrigel invasion assay, respectively. (**H**) Stable overexpression of Mtss-1, Pai-1, Rsu-1, Timp-1, or MPRT does not affect orthotopic tumor growth in nude mice. I, H & E stained lung sections showing metastatic nodules among the different genotype. (**J)** Quantification of the number of lung metastases and percentage of lung area with metastasis (**K**) among different genotypes. Two-tailed student's t-test and one-way ANOVA were used for statistical analysis. All data are mean ± SEM. Scale bars: 100 μm (A). *P<0.05, **P<0.01.

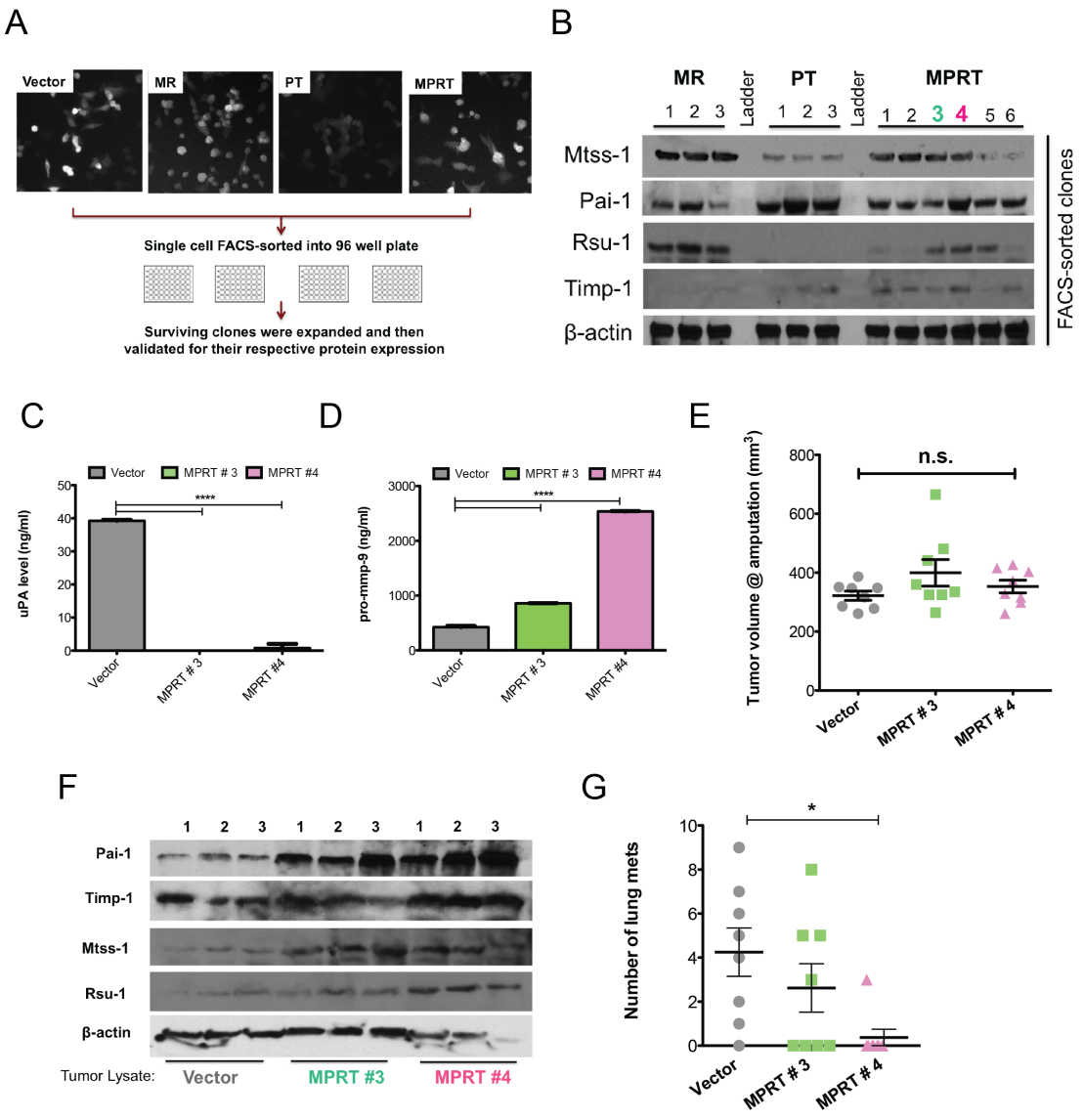

Supplementary Figure 13. Selection and characterization of primary KP; LSL-miR-182 cell line expressing all four miR-182 targets. (**A**) Strategy used to select cells expressing all four targets derived from a single cell clone. (**B**) Western blot confirming ectopic expression of stably transduced target genes in different selected clones. Clones MPRT #3 and MPRT #4 were selected for further experiments. Note: MPRT #4 expresses stable expression of all four targets, but MPRT #3 has weak expression of Timp-1. (**C**) ELISA confirming significant modulation of uPA and pro-MMP-9 (**D**) in both clones MPRT #3 and MPRT #4. (**E**) Stable overexpression of MPRT does not affect orthotopic tumor growth in nude mice. (**F**) Western blot performed on cell lysates from orthotopic sarcomas confirms overexpression of target genes in both clones MPRT #3 and MPRT #4. (**G**) Quantification of the number of lung metastases among different clones. One-way ANOVA were used for statistical analysis. All data are mean ± SEM *P<0.05.

Supplementary Table 1. List of differentially expressed miRNAs between non-metastatic versus metastatic primary mouse sarcomas using miRNA TLDA-array. (Blue color: low expression; Red color: high expression)

microRNA	Fold-	p-value

	change	
mmu-miR-741	0.12	0.030545
mmu-miR-369-5p	0.14	0.001025
mmu-miR-511	0.22	0.00845
mmu-miR-433	0.24	0.003165
mmu-miR-667	0.24	0.005346
mmu-miR-135a	0.25	0.018575
mmu-miR-489	0.3	0.004304
mmu-miR-323-3p	0.33	0.016233
mmu-miR-493	0.33	0.019341
mmu-miR-134	0.34	0.002491
mmu-miR-141	0.34	0.010273
mmu-miR-431	0.34	0.038702
mmu-miR-672	0.36	0.017806
mmu-miR-367	0.36	0.038439
mmu-miR-544	0.37	0.040212
mmu-miR-434-3p	0.38	0.000398
mmu-miR-376a	0.39	0.019064
mmu-miR-409-3p	0.4	0.021962
mmu-miR-495	0.41	0.02367
mmu-miR-539	0.42	0.01817
mmu-miR-337-5p	0.42	0.028233
mmu-miR-331-5p	0.48	0.040726
mmu-miR-410	0.49	0.041912
mmu-miR-136	0.51	0.02367
mmu-miR-411	0.51	0.026027
mmu-miR-223	0.55	0.002796
mmu-miR-574-3p	0.55	0.007661
mmu-miR-193b	0.56	0.006263
mmu-miR-126-3p	0.59	0.000508
mmu-miR-126-5p	0.63	0.027828
mmu-miR-340-3p	0.68	0.017297
mmu-miR-145	0.68	0.023448
mmu-miR-16	0.72	0.017728
mmu-miR-26a	0.77	0.027147
mmu-miR-30d	0.77	0.03994
mmu-miR-532-5p	1.7	0.018311
mmu-miR-532-3p	1.71	0.008108
mmu-miR-182	2.02	0.028035
mmu-miR-677	2.05	0.047643
rno-miR-351	3.1	0.025377
mmu-miR-147	3.3	0.013841
mmu-miR-96	3.42	0.019771

Supplementary Table 2. List of differentially expressed proteins between miR-182 WT and miR-182 deleted primary sarcoma cells from a proteomic screen. Only proteins with a change of 2 fold or more are included in this list.

Table A. Upregulated proteins in miR-182 F/F versus miR-182 WT (Greater than 2-folds change)			
Protein Description	**Peptide Count**	**Fold-change KO versus**	**P-value**

		WT	
ref|NP_064330.2 microsomal glutathione S-transferase 1	2	19.1	0.004
ref|NP_032897.2 plasminogen activator inhibitor 1 precursor	3	12.9	0.024
ref|NP_001191839.1 uncharacterized protein LOC226691	7	12.5	0.005
ref|NP_056598.2 ubiquitin-like protein ISG15 precursor	4	12.5	0.002
ref|NP_032620.2 lactadherin isoform 1 precursor	5	9.7	0.021
ref|NP_783327.2 alpha-2-macroglobulin-P precursor	2	9.2	0.023
ref|NP_034510.3 H-2 class I histocompatibility antigen, L-D alpha chain precursor	7	9.1	2.69E-04
ref|NP_201571.2 solute carrier organic anion transporter family member 2A1	3	8.5	0.003
ref|NP_034858.2 protein-lysine 6-oxidase precursor	4	8.3	0.004
ref|NP_075615.2 ras-related protein Rab-8A	5	8.0	0.021
ref|NP_034459.2 podoplanin precursor	2	7.7	0.006
ref|NP_035767.4 three prime repair exonuclease 1	3	7.6	0.002
ref|NP_032352.1 immunity-related GTPase family M protein 1	6	7.1	0.001
ref|NP_035723.2 metalloproteinase inhibitor 1 precursor	5	6.3	6.23E-04
ref|NP_598567.2 UDP-N-acetylhexosamine pyrophosphorylase	2	6.2	0.021
ref|NP_032018.2 fibulin-2 isoform a precursor	2	6.1	0.034
ref|NP_033408.1 thy-1 membrane glycoprotein preproprotein	4	5.6	0.049
ref|NP_035231.2 protein kinase C alpha type	2	5.6	0.023
ref|NP_075630.2 torsin-3A precursor	5	5.5	0.011
ref|NP_064335.1 signal peptidase complex catalytic subunit SEC11A	4	5.1	0.021
ref|NP_035328.2 prostaglandin G/H synthase 2 precursor	18	4.9	0.006
ref|NP_080831.2 reticulocalbin-3 precursor	9	4.7	0.006
ref|NP_058044.1 peroxiredoxin-4 precursor	11	4.6	0.01
ref|NP_077160.1 glutathione peroxidase 7 precursor	3	4.5	0.004
ref|NP_032357.2 interferon-induced protein with tetratricopeptide repeats 1	14	4.3	7.91E-04
ref|NP_034390.1 interferon-induced guanylate-binding protein 2	6	4.2	8.49E-05
ref|NP_776147.1 apolipoprotein L 9a	3	4.0	0.015
ref|NP_034460.3 embigin precursor	2	3.9	0.03
ref|NP_061208.3 interferon gamma induced GTPase	7	3.8	0.001
ref|NP_071301.2 protein Niban	2	3.8	0.025
ref|NP_067482.4 sulfide:quinone oxidoreductase, mitochondrial	10	3.7	0.006
ref|NP_035148.1 sequestosome-1	5	3.7	0.01
ref|NP_001152773.1 galectin-9 isoform 2	2	3.6	0.006
ref|NP_035642.1 surfeit locus protein 4	4	3.6	0.007
ref|NP_033404.1 thrombomodulin precursor	3	3.5	0.005

ref|NP_001139780.1 drebrin-like protein isoform 1	3	3.5	4.00E-04
ref|NP_035161.2 prolyl 4-hydroxylase subunit alpha-2 isoform 2 precursor	13	3.2	0.015
ref|NP_034631.1 interferon-induced protein with tetratricopeptide repeats 3	6	3.2	0.001
ref|NP_075638.2 cytosolic non-specific dipeptidase	6	3.1	0.011
ref|NP_062757.2 prolyl 3-hydroxylase 1 isoform 2 precursor	2	3.0	0.01
ref|NP_001239582.1 extracellular matrix protein 1 isoform 2 precursor	7	3.0	0.01
ref|NP_080073.1 cytochrome b5	5	2.9	0.003
ref|NP_031817.1 cysteine and glycine-rich protein 1	5	2.9	0.049
ref|NP_001087235.1 myeloid-associated differentiation marker	3	2.9	0.008
ref|NP_031568.2 biglycan precursor	9	2.8	0.017
ref|NP_598890.1 pre-mRNA-processing factor 19 isoform 2	9	2.8	0.04
sp|P02769.4 ALBU_BOVIN Serum albumin	43	2.8	0.008
ref|NP_001153490.1 torsin-1A-interacting protein 1 isoform 1	8	2.8	0.018
ref|NP_112462.1 A-kinase anchor protein 12	6	2.7	0.01
ref|NP_035907.1 zyxin	3	2.7	0.027
ref|NP_032355.2 interferon-activable protein 204	17	2.7	9.23E-04
ref|NP_112444.1 interleukin-1 receptor antagonist protein isoform 1	2	2.7	0.05
ref|NP_033492.1 UDP-glucose 6-dehydrogenase	17	2.6	0.025
ref|NP_082571.1 protein disulfide-isomerase A5 precursor	6	2.6	1.50E-06
ref|NP_035280.1 galectin-3-binding protein precursor	11	2.5	0.02
ref|NP_001020773.1 interleukin-1 receptor-like 1 isoform a precursor	5	2.5	0.012
ref|NP_034342.1 four and a half LIM domains protein 2	4	2.5	0.044
ref|NP_038791.2 transducin beta-like protein 2 precursor	2	2.5	0.039
ref|NP_001177903.1 tyrosine-protein kinase receptor UFO isoform 2 precursor	3	2.5	0.018
ref|NP_035205.1 multidrug resistance protein 1B	7	2.5	0.012
ref|NP_660210.1 2'-5'-oligoadenylate synthase-like protein 1	11	2.5	0.027
ref|NP_032575.2 alpha-mannosidase 2	12	2.4	0.004
ref|NP_835188.2 protein PML isoform 2	2	2.4	0.011
ref|NP_032652.3 C-type mannose receptor 2 precursor	3	2.4	0.036
ref|NP_001164324.1 myeloid cell nuclear differentiation antigen-like protein	4	2.4	0.033
ref|NP_034572.1 heme oxygenase 1	5	2.4	0.025
ref|NP_001152954.1 ras-related protein Rab-34	2	2.3	0.033
ref|NP_473384.1 RNA-binding protein Musashi homolog 2 isoform 1	2	2.3	0.046
ref|NP_038660.1 purine nucleoside phosphorylase	4	2.3	0.042
ref|NP_035160.1 prolyl 4-hydroxylase subunit alpha-1 precursor	21	2.3	0.005
ref|NP_808385.2 uncharacterized protein LOC239673	3	2.3	0.012
ref|NP_001104513.1 serpin H1 precursor	25	2.3	8.69E-

			04
ref|NP_031505.1 ADP-ribosylation factor 4	7	2.2	0.015
ref|NP_848713.1 transgelin-2	12	2.2	0.022
ref|NP_663550.1 caldesmon 1	27	2.2	0.012
ref|NP_031670.1 lysosome membrane protein 2 precursor	2	2.2	0.042
ref|NP_766431.3 torsin-1A-interacting protein 2 isoform b	3	2.1	0.042
ref|NP_001139646.1 ran GTPase-activating protein 1	14	2.1	0.023
ref|NP_766415.1 leucyl-cystinyl aminopeptidase	6	2.1	0.039
ref|NP_033127.1 ras-related protein R-Ras precursor	2	2.1	0.006
ref|NP_032436.1 integral membrane protein 2B	4	2.1	0.019
ref|NP_062782.2 PDZ and LIM domain protein 5 isoform ENH1	7	2.1	0.021
ref|NP_149064.1 keratin, type II cytoskeletal 7	3	2.1	0.006
ref|NP_058077.2 syntaxin-7	5	2.0	0.026
ref|NP_038588.2 heat shock protein beta-1	3	2.0	2.34E-04
ref|NP_001177187.1 ribosomal protein S27-like	2	2.0	0.032
ref|NP_001017959.1 lysosome-associated membrane glycoprotein 2 isoform 1 precursor	6	2.0	0.002
ref|NP_058060.2 integrin beta-3 precursor	2	2.0	0.036
ref|NP_001123951.1 nucleobindin-2 precursor	6	2.0	0.006

Table B. Downregulated proteins in miR-182 F/F versus miR-182 WT (Greater than 2-folds change)

Protein Description	Peptide Count	Fold-change KO versus WT	P-value
ref|NP_776291.1 alanine aminotransferase 2	2	-6.2	0.007
ref|NP_038593.1 integrin alpha-3 precursor	3	-5.9	2.30E-04
ref|NP_075541.1 something about silencing protein 10	2	-3.9	0.043
ref|NP_032563.2 alpha-methylacyl-CoA racemase	2	-3.6	0.004
ref|NP_032278.1 high mobility group protein B2	3	-3.6	0.001
ref|NP_001240686.1 acidic leucine-rich nuclear phosphoprotein 32 family member E isoform 2	2	-3.5	0.011
ref|NP_083139.1 iron-sulfur cluster assembly 2 homolog, mitochondrial precursor	2	-3.4	0.04
ref|NP_473411.2 AFG3-like protein 1	2	-3.3	0.047
ref|NP_598883.1 nurim	2	-3.2	0.04
ref|NP_079829.1 39S ribosomal protein L11, mitochondrial	2	-3.1	0.008
ref|NP_898850.2 insulin-like growth factor 2 mRNA-binding protein 2	6	-2.8	0.012
ref|XP_003945388.1 PREDICTED: high mobility group protein B1-like	7	-2.6	0.02
ref|NP_035351.1 transcriptional activator protein Pur-beta	4	-2.6	0.022

ref|NP_034937.1 MARCKS-related protein	5	-2.6	0.049
ref|NP_081551.2 pentatricopeptide repeat-containing protein 3, mitochondrial precursor	6	-2.5	0.002
ref|NP_031650.3 chromobox protein homolog 3	7	-2.5	0.012
ref|NP_598768.1 CDGSH iron-sulfur domain-containing protein 1	2	-2.4	0.027
ref|NP_080064.3 nucleus accumbens-associated protein 1	2	-2.4	0.048
ref|NP_001164424.1 mRNA cap guanine-N7 methyltransferase isoform 2	2	-2.4	0.016
ref|NP_001074627.1 clustered mitochondria protein homolog	3	-2.3	0.016
ref|NP_001074218.1 general transcription factor II-I isoform 5	7	-2.3	0.008
ref|NP_001103686.1 chromobox protein homolog 5	5	-2.3	0.03
ref|NP_034038.2 N-acylneuraminate cytidylyltransferase	2	-2.2	0.022
ref|NP_766599.2 isocitrate dehydrogenase	23	-2.2	0.015
ref|NP_035932.2 ATP-dependent Clp protease ATP-binding subunit clpX-like, mitochondrial isoform 1	6	-2.2	0.034
ref|NP_080665.1 polymerase delta-interacting protein 2	3	-2.2	0.035
ref|NP_082359.1 chromatin assembly factor 1 subunit B	2	-2.2	0.02
ref|NP_033788.3 aldose reductase	8	-2.2	0.043
ref|NP_291096.2 FACT complex subunit SPT16	7	-2.2	0.04
ref|NP_081480.2 39S ribosomal protein L12, mitochondrial precursor	4	-2.1	0.021
ref|NP_031648.1 chromobox protein homolog 1	3	-2.1	4.86E-04
ref|NP_001116304.1 epidermal growth factor receptor substrate 15-like 1 isoform b	2	-2.1	0.017
ref|NP_080218.1 obg-like ATPase 1 isoform a	4	-2.1	0.013
ref|XP_920204.1 PREDICTED: ribosome biogenesis protein NSA2 homolog isoform 1	2	-2.1	0.043
ref|NP_776292.1 protein RCC2	15	-2.1	0.01
ref|NP_919320.1 ribosome biogenesis protein BMS1 homolog	2	-2.1	0.042
ref|NP_277068.1 ubiquilin-4	2	-2.1	0.025
ref|NP_081278.1 DNA-directed RNA polymerase II subunit RPB4 isoform 1	2	-2.1	0.021
ref|NP_001186199.1 aldolase 1 A retrogene 1	2	-2.1	0.024
ref|NP_081710.1 regulation of nuclear pre-mRNA domain-containing protein 1B	2	-2.1	0.019

Supplementary Table 3. Genes upregulated in the proteomic screen that have miR-182 binding sites.

Upregulated genes in the	Number of miR-182	Investigated in the current	Previously reported as a

proteomic screen with a miR-182 binding motif	binding sites	study	miR-182 target
Lamp-2	1		
Pai-1	1	Yes	No
Timp-1	1	Yes	No
Pdpn	1		
Fstl-1	1		
Pgs-1	1		
Bnip-3	1	Yes	No
Arf-4	2		
*Rsu-1	1	Yes	No
**Mtss-1	3	Yes	Yes

* Rsu-1 was upregulated ~1.4 fold in the proteomic screen. ** Mtss-1 was not detected in proteomic screen.

Supplementary Table 4. Sequences of all the primers used in the study.

Name	Direction	Sequence	Use
miR-182-loxp-fwd	Forward	CATCCCAGGGTCTGTGTGTC	Genotyping
miR-182-loxp-rev	Reverse	CAGCATGAGTGTTTTATGAG	Genotyping
miR-182-4-rev	Reverse	GTCATCTGGAGCTGCGGCCT	Genotyping

R26F2	Forward	CTCGGCTAGGTAGGGGATCG	Genotyping
D274	Forward	TTCGTGCAAGTTGAGTCCATC	Genotyping
L15	Reverse	TACGGGGTCATTAGTTCA	Genotyping
D229	Reverse	GCTCCTTTTACGCTATGTGG	Genotyping
miR-182-Fwd-Nsi1	Forward	ATGCATGACCATACAGGCC GAAGGAC	Cloning
miR-182-Rev-Mlu1	Reverse	ACGCGTCATCTGTCTCTCCCTC ACCAAG	Cloning
miR-182-pcdh-fwd	Forward	CTAGAGCTAGCGAATTCGACCATACAGGCCGAAG	Cloning
miR-182-pcdh-rev	Reverse	CAGATCCTTGCGGCCGC CATCTGTCTCTCCCTC	Cloning
miR-96-pcdh-fwd	Forward	CTAGAGCTAGCGAATTCGTGTGACTCCTGTCCTG	Cloning
miR-96-pcdh-rev	Reverse	CAGATCCTTGCGGCCGCCCGCAAGCATCTCCATC	Cloning
Rsu-1-pcdh-fwd	Forward	CTAGAGCTAGCGAATTCATGTCCAAGTCACTGAA	Cloning
Rsu-1-pcdh-rev	Reverse	GCAGATCCTTGCGGCCGCTCATTTGTTCTTGGC	Cloning
Mtss-1-pcdh-fwd	Forward	CTAGAGCTAGCGAATTCATGGAGGCTGTGATCGA	Cloning
Mtss-1-pcdh-rev	Reverse	GCAGATCCTTGCGGCCGCCTAAGAGAAGCGCGG	Cloning
Rasa-1-3'utr-pgl3-	Forward	GATCGCCGTGTAATTCTAGACAGCCTGTGTTCTG	Cloning
Rasa-1-3'utr-pgl3-	Reverse	CCGGCCGCCCCGACTCTAGACCTTGTATACAATA	Cloning
Rsu-1-3'utr-pgl3-fwd	Forward	GAT CGC CGT GTA ATT CTA GAG AAC AAATGA	Cloning
Rsu-1-3'utr-pgl3-rev	Reverse	CCG GCC GCC CCG ACT CTA GAGTTA AAT GAA	Cloning
Mtss-1-3'utr-pgl3-	Forward	GAT CGC CGT GTA ATT CTA GACTGGTTC CCA	Cloning
Mtss-1-3'utr-pgl3-rev	Reverse	CCG GCC GCC CCG ACT CTA GACTTT ATT TAT	Cloning
L1cam-3'utr-pgl3-	Forward	GATCGCCGTGTAATTCTAGAGCAAGGTCCAGCCA	Cloning
L1cam -3'utr-pgl3-	Reverse	CCGGCCGCCCCGACTCTAGACATTTCTAGGTTTT	Cloning
Rassf1a-3'utr-pgl3-	Forward	GATCGCCGTGTAATTCTAGACAGTGCAAAG	Cloning
Rassf1a-3'utr-pgl3-	Reverse	CCGGCCGCCCCGACTCTAGATGATGCCTGA	Cloning
Pai-1-3'utr-pgl3-fwd	Forward	GATCGCCGTGTAATTCTAGACAGTGGGAAGAGAC	Cloning
Pai-1-3'utr-pgl3-rev	Reverse	CCGGCCGCCCCGACTCTAGAGTTTGCATATTCTC	Cloning
Timp-1-3'utr-pgl3-	Forward	GATCGCCGTGTAATTCTAGAGACCTGAAGCCTTC	Cloning
Timp-1-3'utr-pgl3-	Reverse	CCGGCCGCCCCGACTCTAGAGCTGCTGTCTGAT	Cloning
Timp-2-3'utr-pgl3-	Forward	GATCGCCGTGTAATTCTAGAGAAGGCTGACAGAG	Cloning
Timp-2-3'utr-pgl3-	Reverse	CCGGCCGCCCCGACTCTAGAGAAGAGTGGCTGT	Cloning
Bnip-3-3'utr-pgl3-	Forward	GATCGCCGTGTAATTCTAGAGATGAAGATTTGGA	Cloning
Bnip-3-3'utr-pgl3-rev	Reverse	CCGGCCGCCCCGACTCTAGACACCTATTGACTAT	Cloning
Mtss-1-mut-fwd	Forward	GTTAATATAAACTGATGCAAAATTCAATGTAG	Cloning
Mtss-1-mut-rev	Reverse	CTACATTGAATTTTGCATCAGTTTATATTAAC	Cloning
Rsu-1-mut-fwd	Forward	GTTTCCTTAAAATTCCCCAAGGCAGAAAAC	Cloning
Rsu-1-mut-rev	Reverse	GTTTTCTGCCTTGGGGAATTTTAAGGAAAC	Cloning
Pai-1-mut-fwd	Forward	CCTTAGGGACCTAGCCATGGTGATGCTTGG	Cloning
Pai-1-mut-rev	Reverse	CCAAGCATCACCATGGCTAGGTCCCTAAGG	Cloning
Timp-1-mut-fwd	Forward	GGTGAAATAAAGAACTAAAAGACAAAAGCAA	Cloning
Timp-1-mut-rev	Reverse	TTTGCTTTTGTCTTTTAGTTCTTTATTTCACC	Cloning

Supplementary Table 5. Description of antibodies used in the study.

Antibody (Ab)	Manufacturer	Primary Ab dilution	Secondary Ab (dilution)	Application

Pai-1	Cell Signaling Technology	1:1000	Rabbit (1:5000)	Western blotting
Timp-1	Pierce	1:2000	Mouse (1:5000)	Western blotting
Timp-2	Abcam	1:500	Rabbit (1:5000)	Western blotting
Timp-3	Abcam	1:500	Rabbit (1:5000)	Western blotting
Rsu-1	Sigma	1:2000	Rabbit (1:5000)	Western blotting
Mtss-1	Cell Signaling Technology	1:2000	Rabbit (1:5000)	Western blotting
uPA	Abcam	1:500	Rabbit (1:5000)	Western blotting
uPAR	R & D sciences	1:500	Mouse (1:5000)	Western blotting
MMP-2	Cell Signaling Technology	1:2000	Rabbit (1:5000)	Western blotting
MMP-9	Sigma	1:2000	Mouse (1:5000)	Western blotting
Bnip-3	Cell Signaling Technology	1:2000	Rabbit (1:5000)	Western blotting
Foxo-3	Epitomics	1:2000	Rabbit (1:5000)	Western blotting
β-actin	BD sciences	1:5000	Mouse (1:10000)	Western blotting
β-catenin	Cell Signaling Technology	1:5000	Mouse (1:10000)	Western blotting
H3	Cell Signaling Technology	1:5000	Rabbit (1:10000)	Western blotting
Digoxin-AP	R & D sciences	1:500	Rabbit (1:500)	In situ hybridization
Ki67	BD sciences	1:500	Rabbit (1:1000)	Immunohistochemistry
Foxo-1	Cell Signaling Technology	1:2000	Rabbit (1:5000)	Western blotting
Vimentin	Cell Signaling Technology	1:1000 WB and 1:100 FC	Rabbit (1:5000 WB and 1:200 F)	Western blotting Flow cytometry

Supplementary Table 6: A significant negative correlation between miR-182 and Pai-1 or Rsu-1 (Spearman (r) correlation test was used for statistical analysis)

	Spearman Correlation (r)	**P-value**

miR-182 & Pai-1	-0.41	0.031
miR-182 & Rsu-1	-0.64	0.0005

Supplementary Methods

Migration & Invasion assay

The 24-Multiwell FluoroBlok Insert System, with a 24-well plate and lid and pore size of 8.0 μm (BD Biosciences, San Jose, CA) was used to determine the effect of

overexpressed miRNAs on migration and invasiveness per the manufacturer's protocol. Infected cells were serum starved overnight, trypsinized the next day, resuspended in serum free medium and then transferred to the hydrated matrigel chambers (~25,000 cells/well). The chambers were then incubated for 24 hrs in DMEM supplemented with 10% FBS in the bottom chambers before examination. The cells on the upper surface were scraped and washed away while the invaded cells on the lower surface were stained with Calcein AM dye for 1h at 37°C. Finally, invaded cells were counted under a microscope, and the relative number was calculated. All the fluoroscence images were taken with 10X objective using Zeiss Axiovert 25 microscope.

Flow cytometry of YFP^+ CTCs

KPY; miR-182 F/F or miR-182 WT control mice with sarcoma were anesthetized. Peripheral blood was collected from the inferior vena cava (IVC) and then mixed with PBS containing 5 mM EDTA. Red blood cells (RBCs) were separated from peripheral blood mononuclear cells (PB-MNCs) using Ficoll-Plaque (GE) according to the manufacturer's instructions. In addition, primary tumors and lungs were digested using collagenase, dispase and trypsin for a minimum of one hour. The digested mixture/slurry was then filtered using a 70-micron filter followed by RBC lysis using ACK buffer (Lonza, Walkersville, MD) according to the manufacturer's protocol. PB-MNCs and cells from tumor & lung were stained with phycoerythrin (PE)-conjugated anti-mouse CD45 IgG (eBioscience) and 7AAD (BD Pharmingen). Data were collected from at least 30,000 PB-MNCs by FACSCanto (BD Pharmingen) and analyzed by Flowjo software (Tree Star, Inc). Statistical significance between two groups was determined by Mann-Whitney test.

Luciferase assay

293T cells were seeded in triplicate in 12-well plates and transfected with different luciferase reporters and Renilla luciferase using the Lipofectamine transfection reagent (Invitrogen) per the manufacturer's protocol. The cells were harvested 24 h later, and a luciferase assay was performed according to the manufacturer's protocol (Promega). Renilla luciferase activity was used as an internal control for transfection efficiency.

Western blotting

Cultured cells or primary tumors were harvested using RIPA lysis buffer and proteins were extracted. The protein concentration was determined using a BCA protein assay kit (Pierce, Thermo Scientific) and samples were separated in SDS polyacrylamide gels (4-20% gradient concentrations) from Bio-Rad (Hercules, CA). After blocking the membrane with 10% milk for one hour, the membrane was probed with a primary antibody (Supplementary Table 4) overnight and subsequently incubated with an HRP-conjugated secondary antibody for one hour. Working solutions of the Pierce ECL Substrate was then added to the membrane for 4 minutes. The membrane was exposed to Thermo Scientific CL-XPosure Film and developed using an X-ray film developer.

After converting X-ray films to computer files, the bands were quantified using *ImageJ* software.

Enzyme linked Immunosorbent assay (ELISA)

Serum-free supernatant from overnight-cultured cells was collected or protein lysates were extracted from primary tumors. Protein concentration was determined using a BCA protein assay kit (Pierce, Thermo Scientific). 1ug of protein was taken for ELISA measurements for uPA and pro-MMP-9. The active uPA protein was determined using a commercially available ELISA Kit as per the manufacturer's protocol (Molecular innovations, MI). Relative absorbance was plotted onto a standard curve to quantify uPA protein. Pro-MMP-9 protein levels were quantified using an ELISA kit from R&D systems (Minneapolis, MN USA). The assay detects only the pro or inactive form of MMP-9, but not the active MMP-9. A standard curve was first plotted and Pro-MMP-9 protein levels were compared to the standard curve.

Experimental metastasis assays

Male athymic nude (nu/nu) mice (ages 4–5 wk) were purchased from Taconic labs (NCRNU-M) and maintained in Duke University's accredited animal facility. To directly assess lung colonization, 100,000 exponentially growing KP-vector or KP-anti-miR-182 cells were injected into nude mice through the tail vein. Two weeks after injection, the animals were sacrificed. The lungs were harvested and fixed in 10% formalin solution, and both the number of tumor nodules and the area of lung with metastases were calculated.

Transduction

The lentiviral vectors (System Biosciences) expressing miR-182, miR-96 or lenti-anti-miR-182 were packaged and used to infect KP cell lines. For in vivo rescue experiments, a sarcoma cell line overexpressing miR-182 from a KP; LSL-miR-182 mouse was infected with a lentivirus expressing a single target or a pool of all four viruses together (MPRT: Clones that express the combination of all four-target genes i.e. Mtss-1, Pai-1, Rsu-1 and Timp-1). Because cells infected with multiple viruses may not lead to overexpression of all four targets in every cell, we also subcloned the MPRT pooled cells by flow cytometry to identify single cell-derived clones that overexpressed all the four miR-182 targets by western blot. All the fluoroscence images were taken with 10X objective using Zeiss Axiovert 25 microscope.

Real-time RT-PCR

RNA from cell lines or the tumors was isolated with Trizol reagent (Invitogen), according to the manufacturer's protocol. Reverse transcription for specific mature miRNAs was performed using the Taqman MicroRNAs Reverse Transcription kit followed by

quantitative PCR with their respective probes, per manufacturer's suggestion (Applied Biosystems, Foster City, CA,). Mature miRNA expression in mouse tumors was calculated using the delta-delta-CT method after normalization to SnoRNA202 expression. Pai-1, Timp-1, Rsu-1, Mtss-1 and Bnip-3 mRNA expression were measured using gene specific Taqman probes purchased from Applied Biosystems. Relative change was measured using the delta-delta-CT method after normalizing gene expression with Gapdh expression.

Northern blotting

15-20 ug RNA from cell lines was separated in a 10% denaturing acrylamide gel purchased from (Bio-Rad, Hercules, CA). Separated RNA was then wet transferred onto the Nylon membrane (N+ Bond, GE Health sciences, Pittsburgh, PA). miR-182, miR-203 and U6 probes (Exiqon, MA) were labeled at the 5' end with radioactive ^{32}P using T4 PNK (New England Biolabs, MA) using the manufacturer's protocol and subsequently cleaned with a Microspin G-25 column (GE Health sciences, Pittsburg, PA). After UV cross-linking, the blot was pre-hybridized for 30 mins and then incubated with the radioactive probe overnight at 55 °C in a hybridization oven. Washing was performed the next day and the membrane was exposed to X-ray film in the dark at -80 °C for 2 hrs.

Full unedited gel for Figure 2A

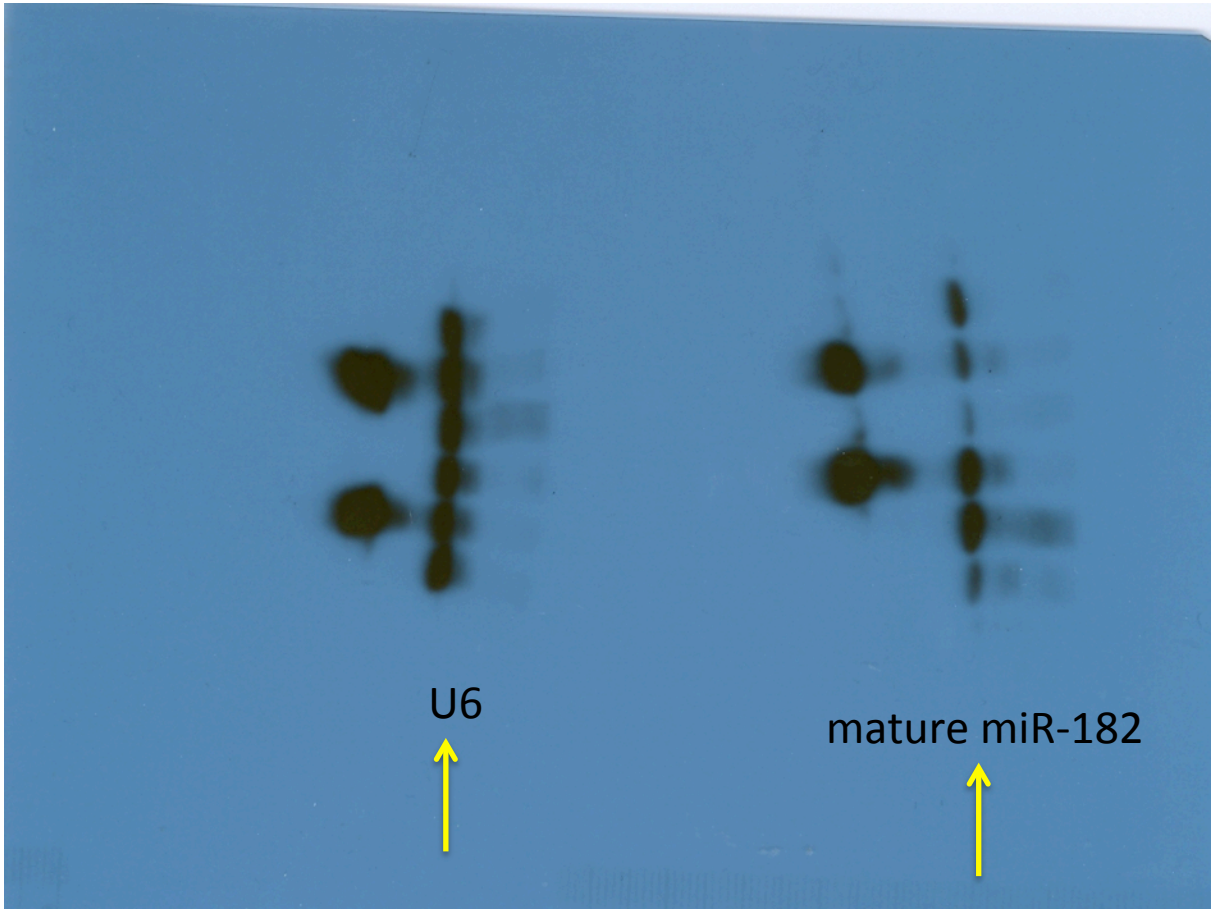

Full unedited gel for Figure 2D

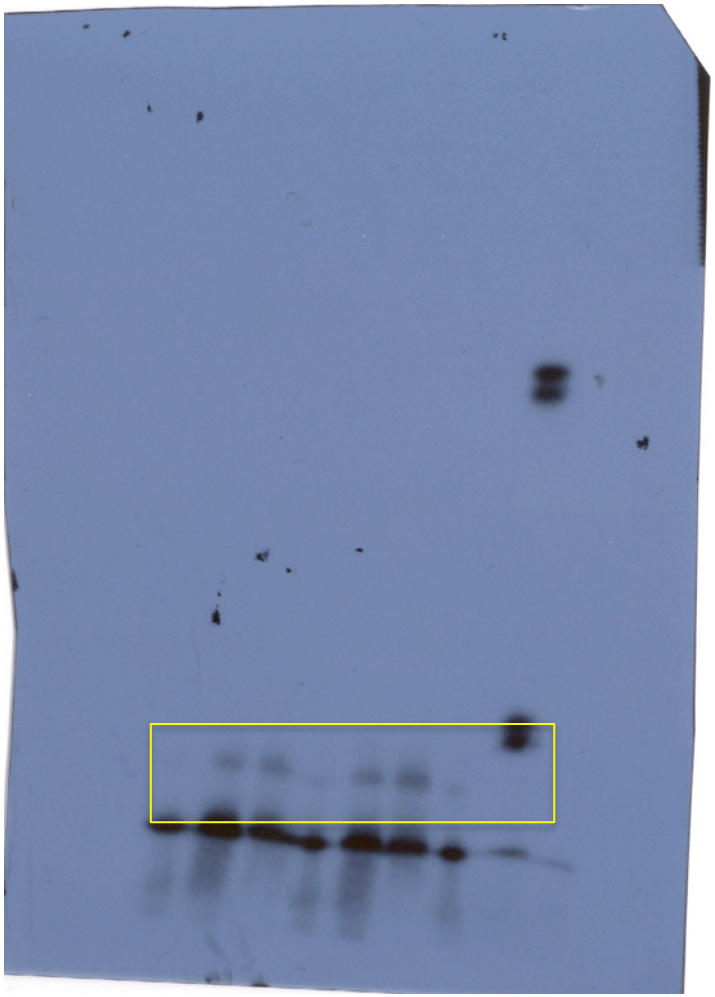

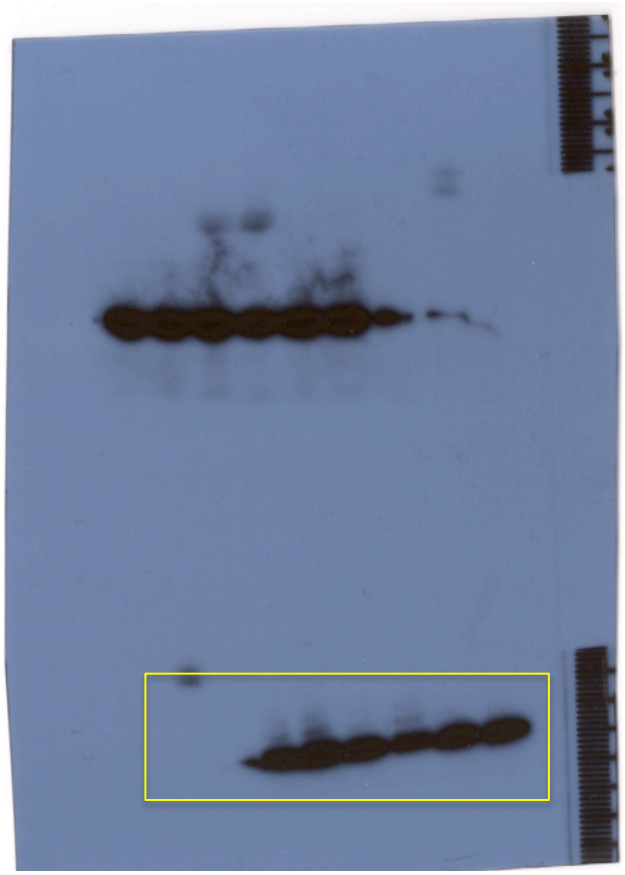

Figure 2H

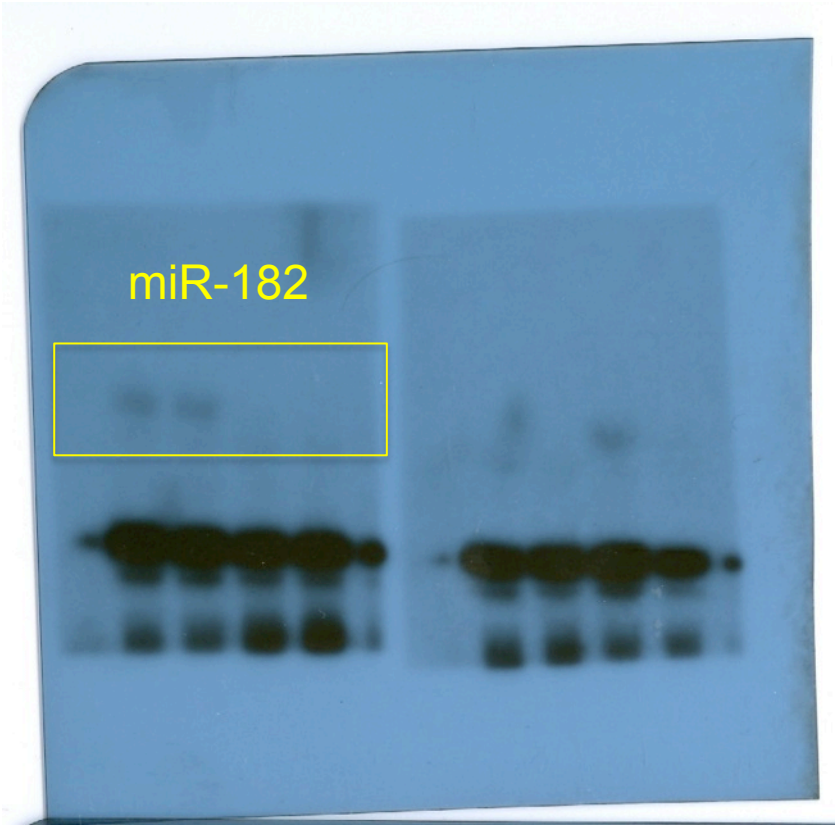

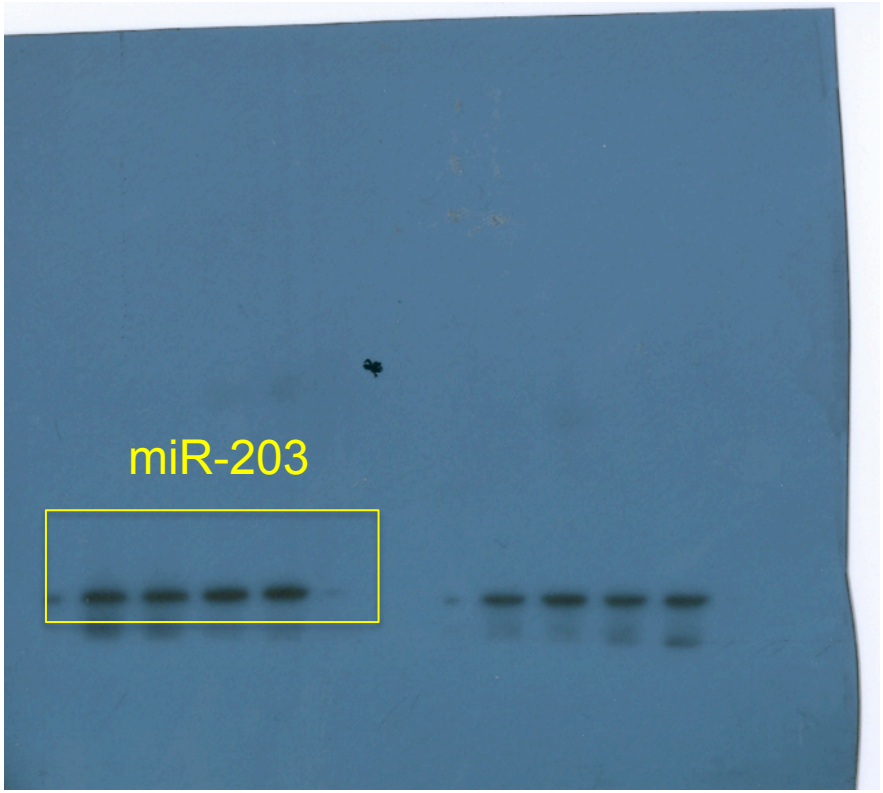

Full unedited gel for Figure 3A

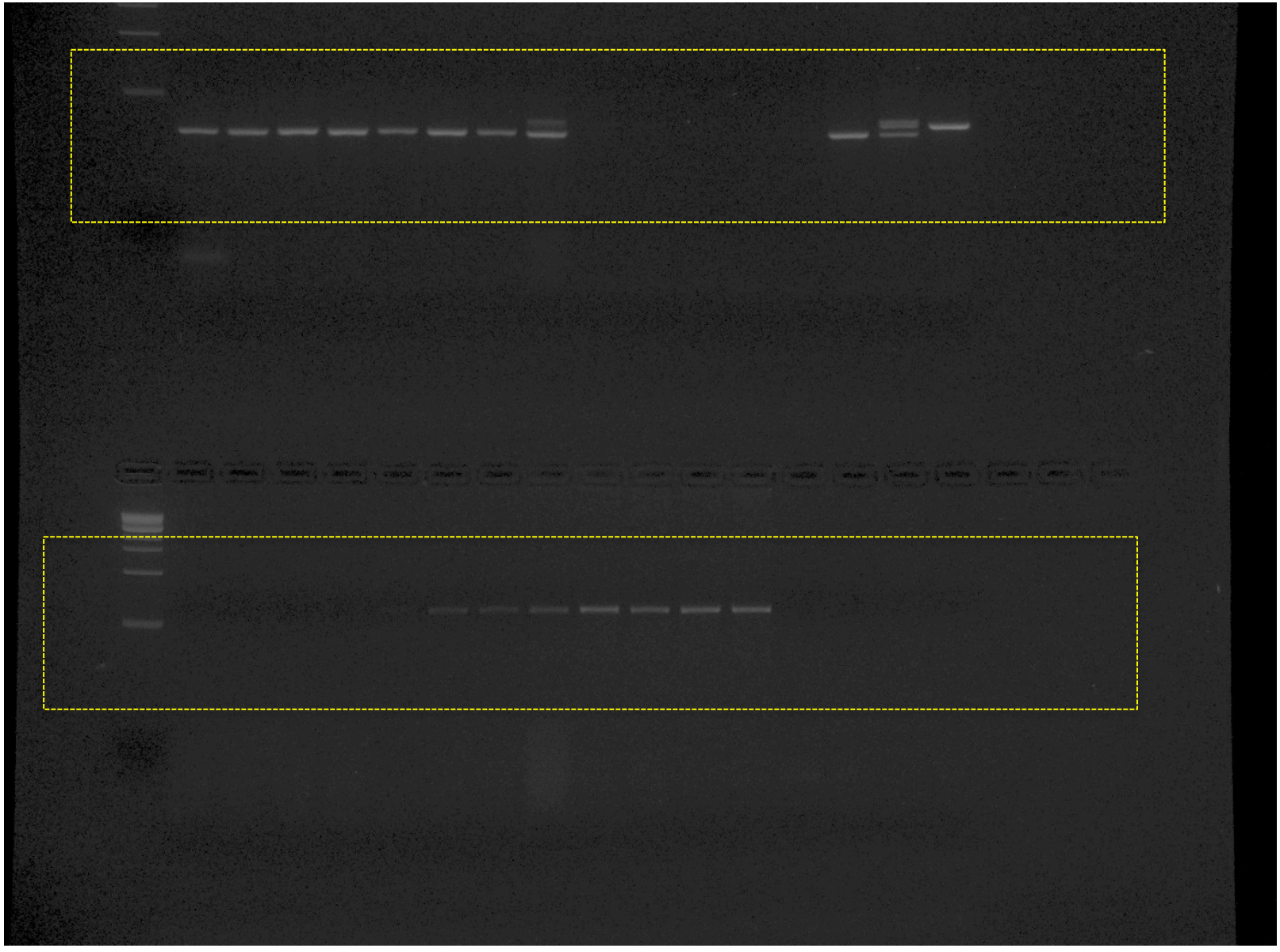

Full unedited gel for Figure 3C

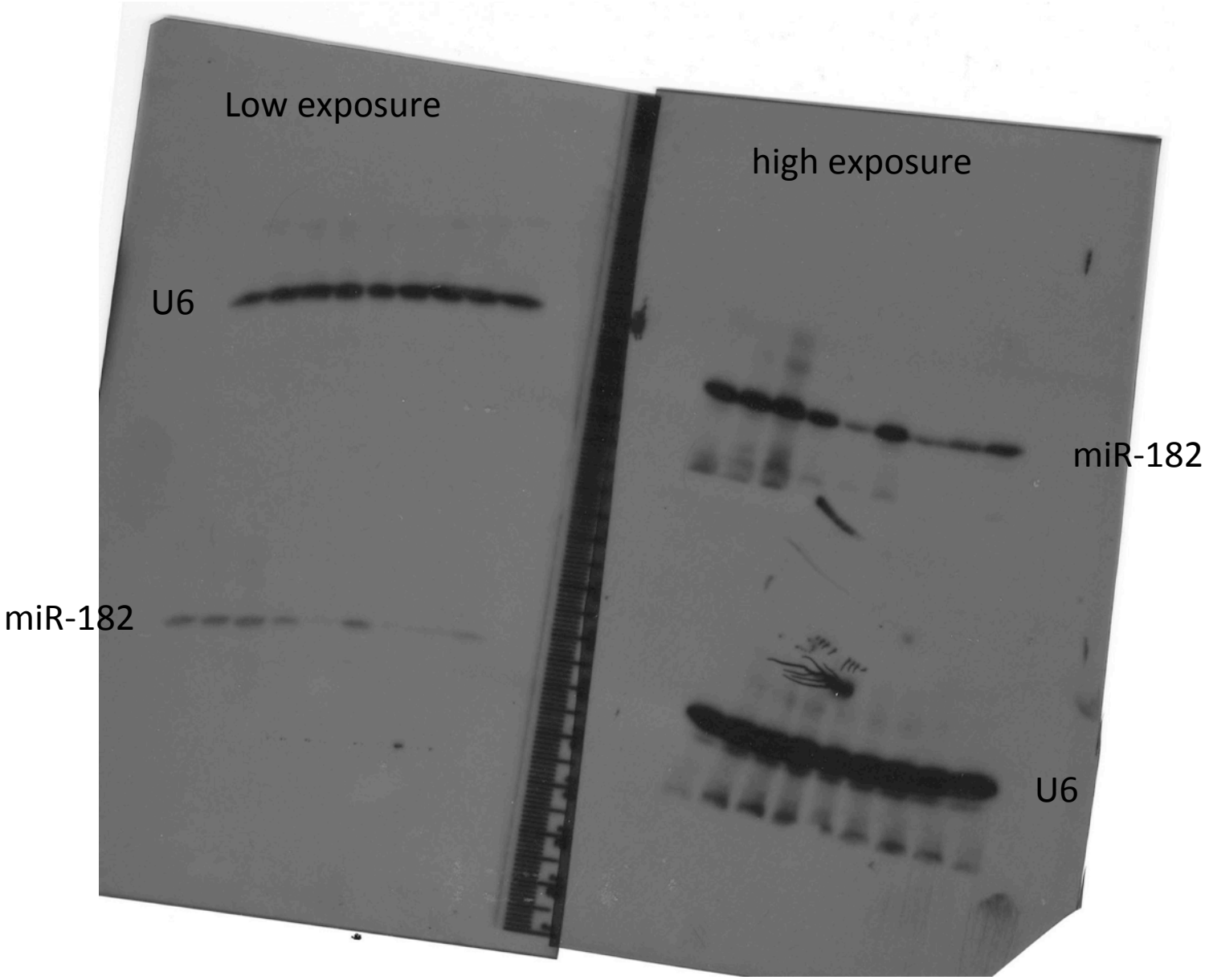

Figure 4A

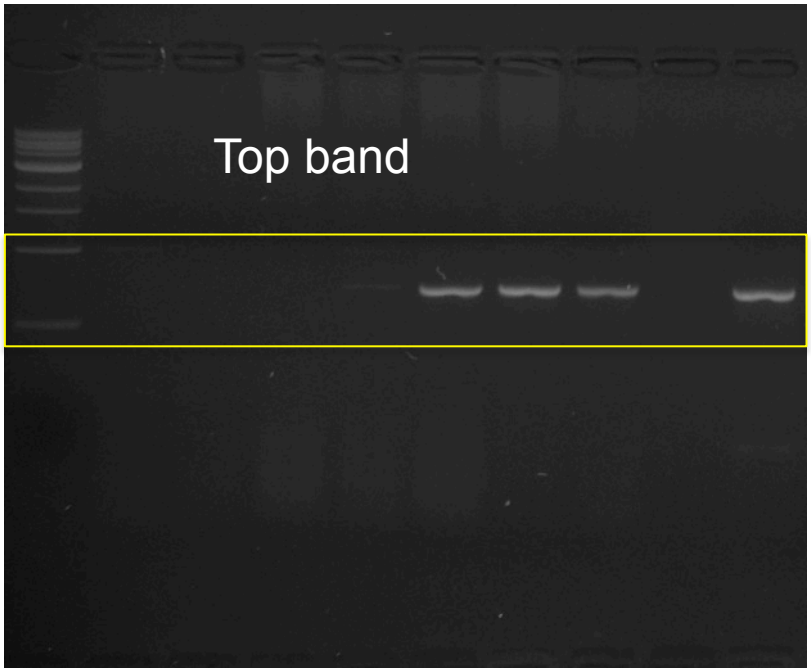

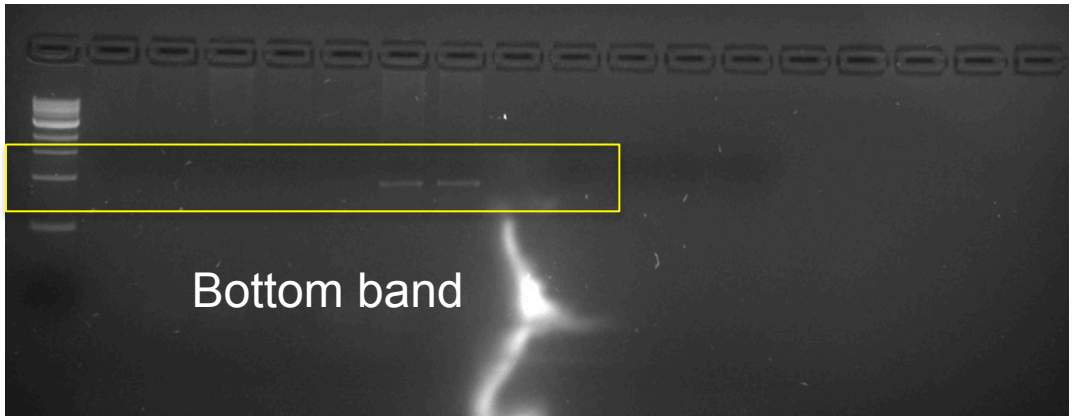

Full unedited gel for Figure 4C

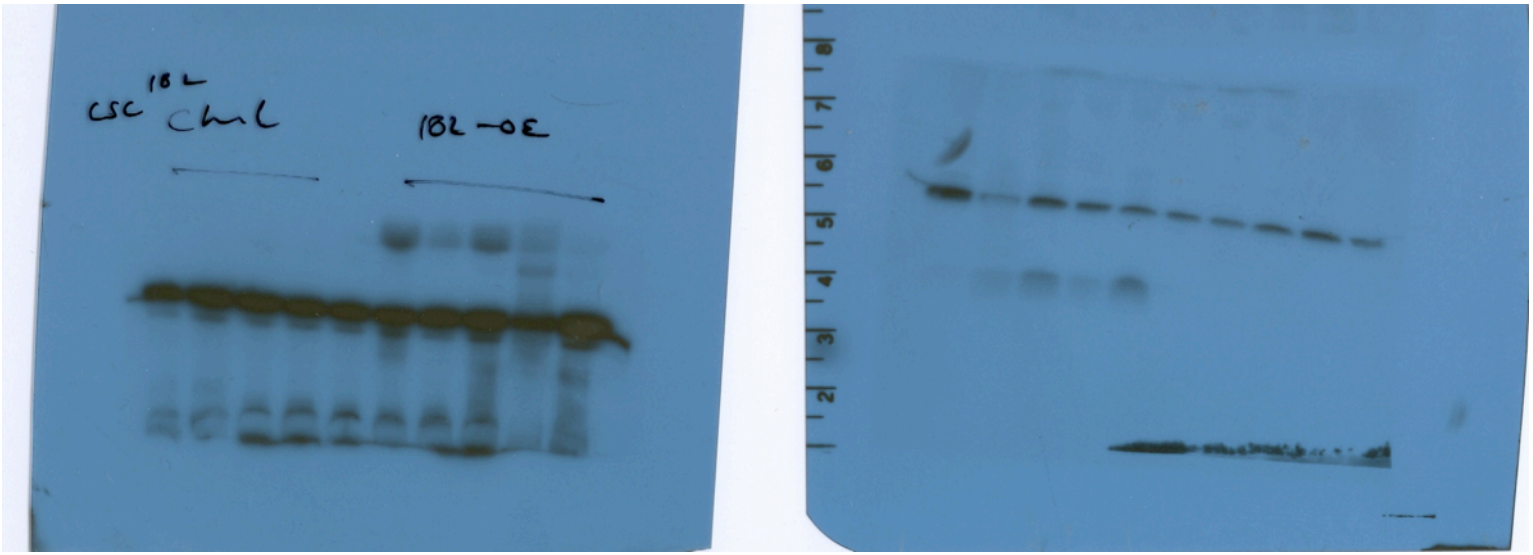


miR-182 5’ lox-P
P53 recombined

Figure 5G

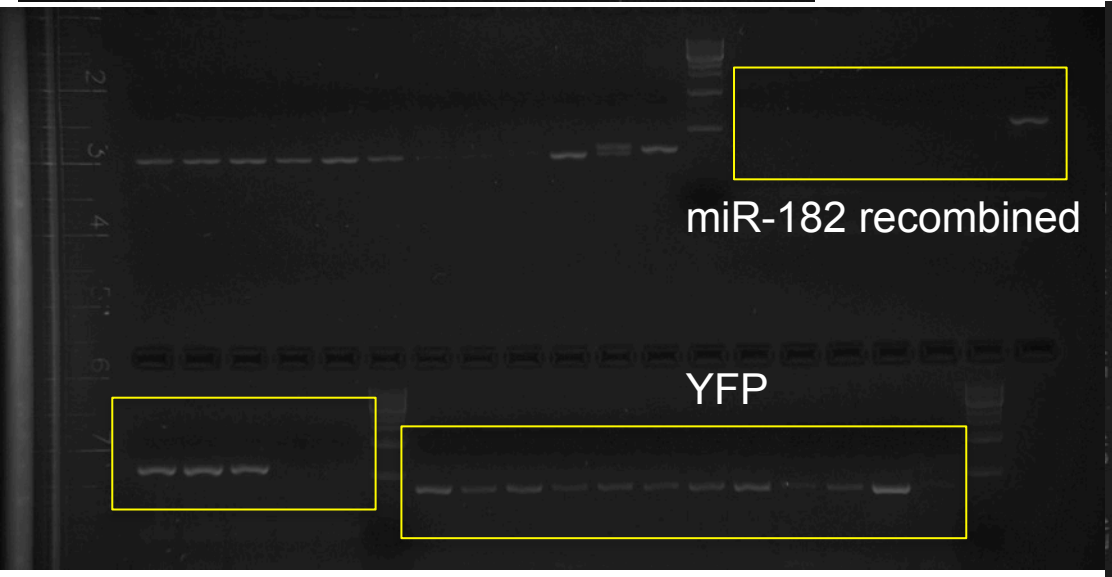
miR-182 recombined
YFP

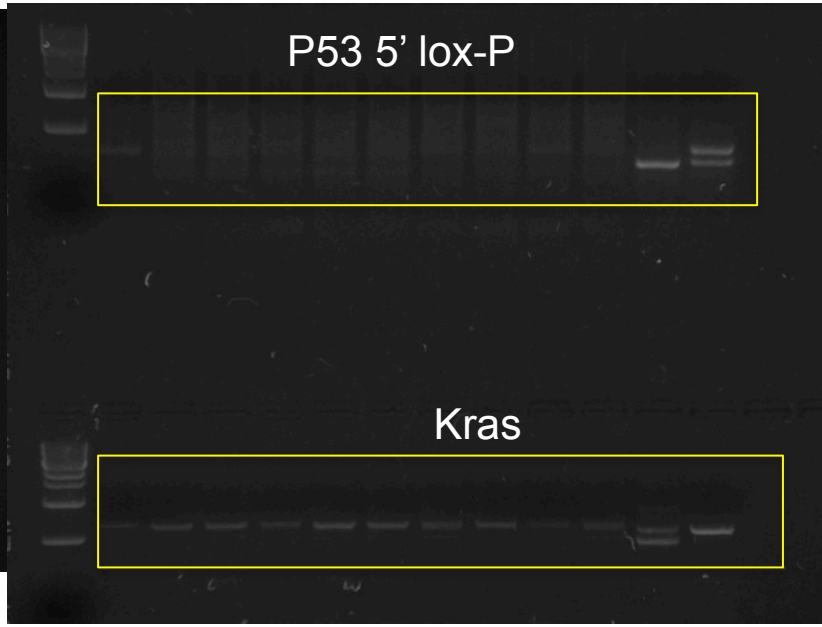
P53 5’ lox-P
Kras

Full unedited gel for Figure 6D

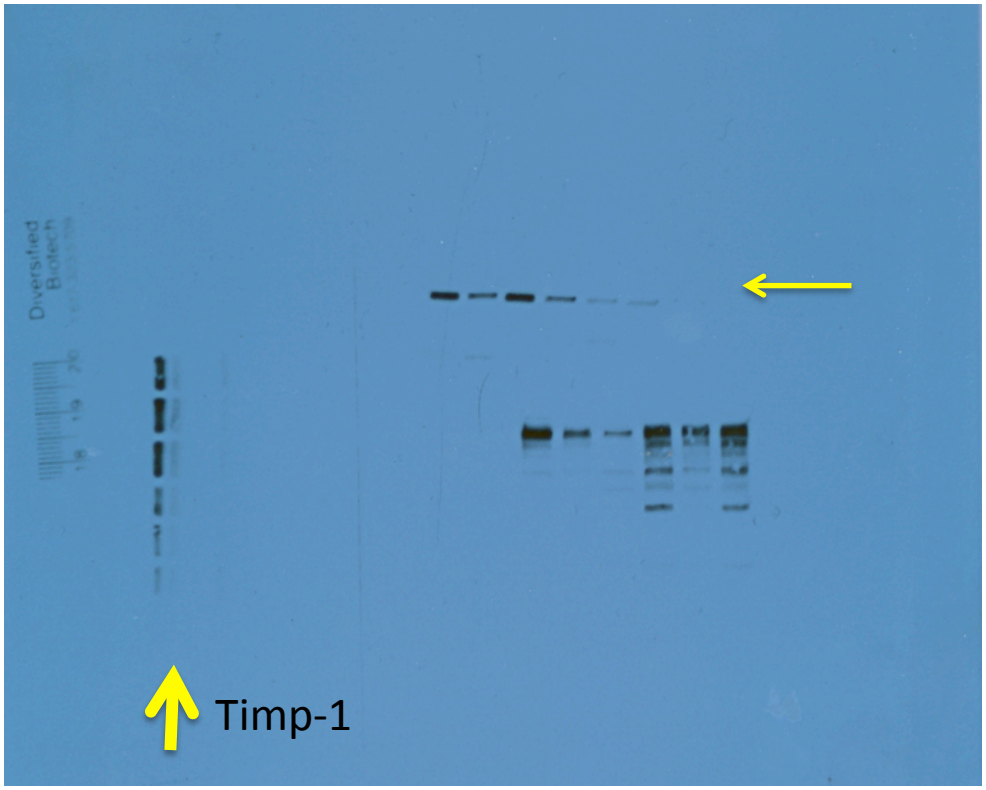

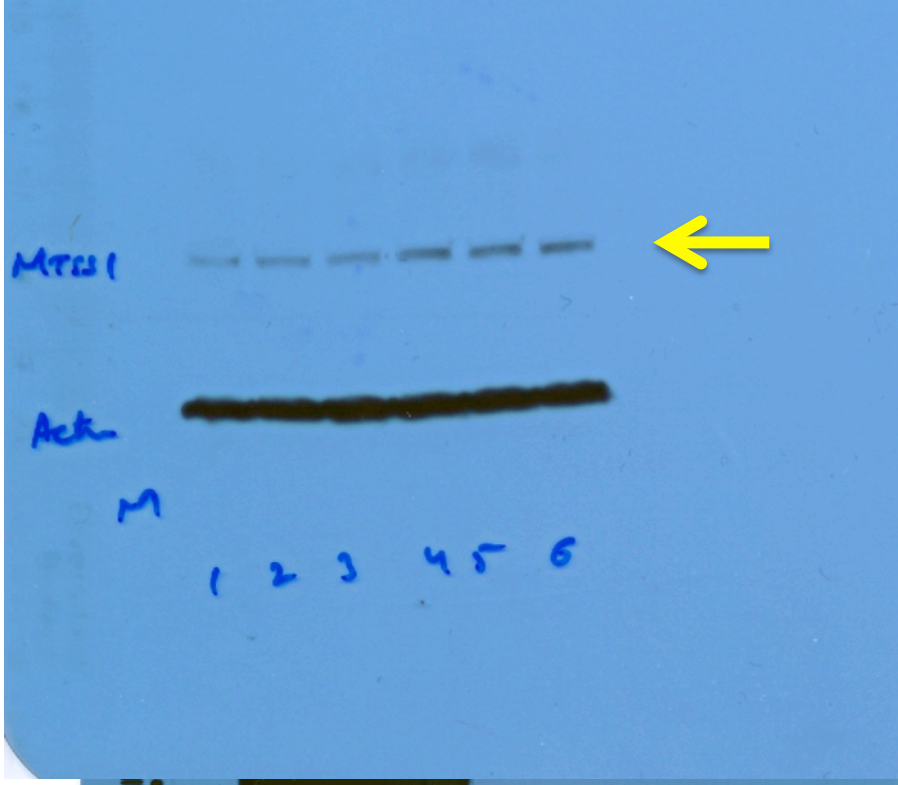

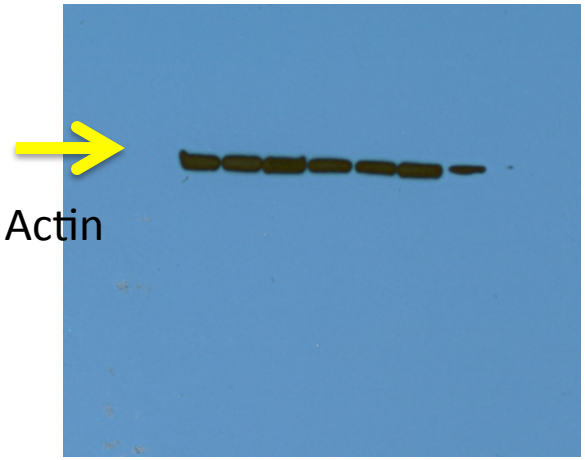

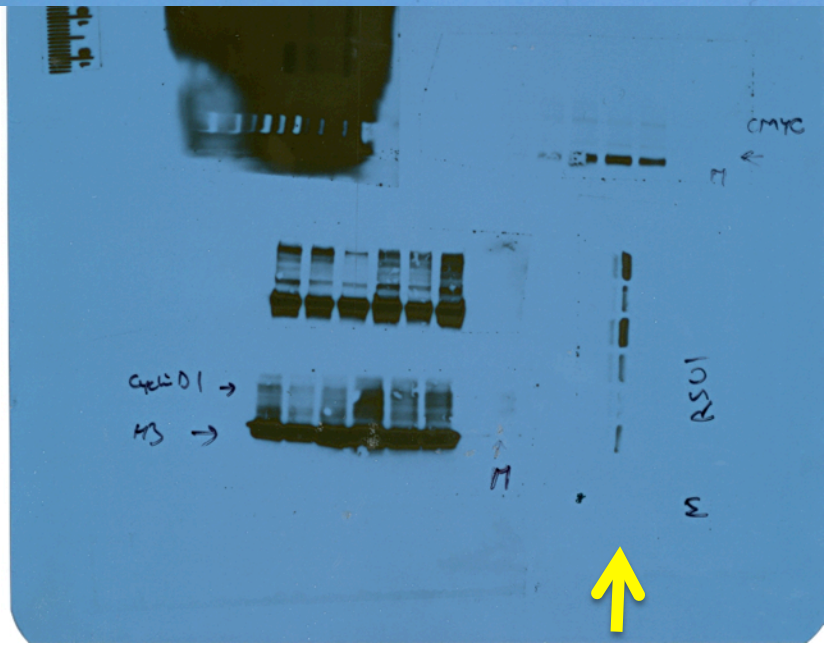

Full unedited gel for Figure 6F